Report

Cell Reports

# Intestinal Dysbiosis and Biotin Deprivation Induce Alopecia through Overgrowth of *Lactobacillus murinus* in Mice

## Graphical Abstract

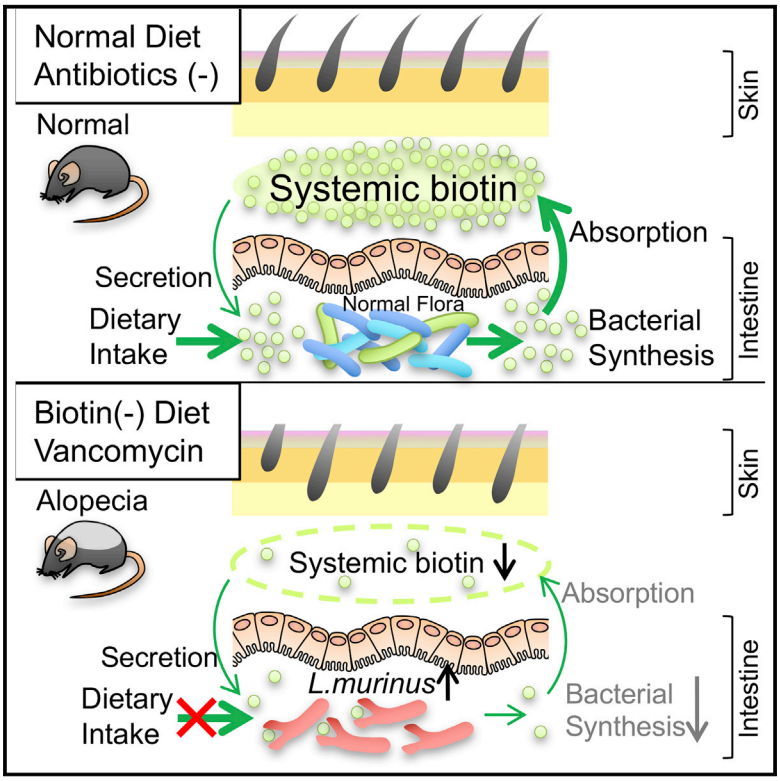


## Highlights

- Antibiotic-induced dysbiosis promotes alopecia in mice fed a biotin-deficient diet
- Vancomycin treatment results in overgrowth of *Lactobacillus murinus*
- *Lactobacillus murinus* consumes and reduces available biotin in the gut
- *Lactobacillus murinus* promotes alopecia in a biotin-dependent manner

## Authors

Atsushi Hayashi, Yohei Mikami, Kentaro Miyamoto, ..., Masayuki Amagai, Manabu Ohyama, Takanori Kanai

## Correspondence

takagast@z2.keio.jp

## In Brief

Gut microbiota metabolism affects host physiology beyond the gastrointestinal tract. Here, Hayashi et al. find that antibiotic-induced gut dysbiosis leads to the development of alopecia in mice on a biotin-deficient diet.

Hayashi et al., 2017, Cell Reports *20*, 1513–1524
August 15, 2017 
http://dx.doi.org/10.1016/j.celrep.2017.07.057

Cell Reports
Report



# Intestinal Dysbiosis and Biotin Deprivation Induce Alopecia through Overgrowth of *Lactobacillus murinus* in Mice

Atsushi Hayashi,[1,2,12] Yohei Mikami,[1,12] Kentaro Miyamoto,[1,2] Nobuhiko Kamada,[3] Toshiro Sato,[1] Shinta Mizuno,[1] Makoto Naganuma,[1] Toshiaki Teratani,[1] Ryo Aoki,[1,4] Shinji Fukuda,[5] Wataru Suda,[6,7] Masahira Hattori,[7,8] Masayuki Amagai,[9,10] Manabu Ohyama,[9,11] and Takanori Kanai[1,10,13,*]

[1]Division of Gastroenterology and Hepatology, Department of Internal Medicine, Keio University School of Medicine, Tokyo 160-8582, Japan
[2]Research Laboratory, Miyarisan Pharmaceutical Co., Ltd., Tokyo 114-0016, Japan
[3]Division of Gastroenterology, Department of Internal Medicine, University of Michigan Medical School, Ann Arbor, MI 48109, USA
[4]Institute of Health Sciences, Ezaki Glico Co., Ltd., Nishiyodogawa, Osaka 555-8502, Japan
[5]Institute for Advanced Biosciences, Keio University, Tsuruoka, Yamagata 997-0052, Japan
[6]Department of Microbiology and Immunology, Keio University School of Medicine, Tokyo 160-8582, Japan
[7]Graduate School of Frontier Sciences, University of Tokyo, Chiba 227-8561, Japan
[8]Graduate School of Advanced Science and Engineering, Waseda University, Tokyo 169-8555, Japan
[9]Department of Dermatology, Keio University School of Medicine, Tokyo 160-8582, Japan
[10]Japan Agency for Medical Research and Development, CREST, Chiyoda-ku, Tokyo 100-0004, Japan
[11]Department of Dermatology, Kyorin University School of Medicine, Tokyo 181-8611, Japan
[12]These authors contributed equally
[13]Lead Contact
*Correspondence: takagast@z2.keio.jp
http://dx.doi.org/10.1016/j.celrep.2017.07.057

## SUMMARY

**Metabolism by the gut microbiota affects host physiology beyond the gastrointestinal tract. Here, we find that antibiotic-induced dysbiosis, in particular, overgrowth of *Lactobacillus murinus* (*L. murinus*), impaired gut metabolic function and led to the development of alopecia. While deprivation of dietary biotin per se did not affect skin physiology, its simultaneous treatment with vancomycin resulted in hair loss in specific pathogen-free (SPF) mice. Vancomycin treatment induced the accumulation of *L. murinus* in the gut, which consumes residual biotin and depletes available biotin in the gut. Consistently, *L. murinus* induced alopecia when monocolonized in germ-free mice fed a biotin-deficient diet. Supplementation of biotin can reverse established alopecia symptoms in the SPF condition, indicating that *L. murinus* plays a central role in the induction of hair loss via a biotin-dependent manner. Collectively, our results indicate that luminal metabolic alterations associated with gut dysbiosis and dietary modifications can compromise skin physiology.**

## INTRODUCTION

The gut microbiota plays critical roles in host physiological processes in the gastrointestinal (GI) tract (Atarashi et al., 2013; Hand, 2016; Ivanov et al., 2008; Kamada and Núñez, 2013; Sommer and Bäckhed, 2013). In addition to this important role in the intestine, recent evidence indicates that the gut microbiota also contributes to physiological regulation in extra-intestinal sites, including the liver, lung, skin, and brain, and its disruption may lead to disease aggravation at individual sites (De Minicis et al., 2014; Hand, 2016; Kamada et al., 2013; Lee et al., 2011; Olszak et al., 2012; Scher et al., 2015). However, the precise mechanisms by which the gut microbial communities regulate the pathophysiology of extra-intestinal sites remain unclear.

The metabolic function of the gut microbiota plays a key role in the maintenance of host homeostasis. Resident microbes in the GI tract harbor genes encoding digestive enzymes lacking in the mammalian host, thereby providing essential micronutrients (e.g., vitamin K, vitamin B12, biotin, niacin, and folic acid) for host homeostasis (Hill, 1997; Said and Mohammed, 2006; Singh et al., 2014). Gut dysbiosis perturbs the metabolic functions of resident microbes, thus contributing to further host metabolic dysfunction (Kau et al., 2011). Biotin (vitamin B7) is a water-soluble vitamin and one of the nutrients that are highly dependent on bacterial production. It is an essential nutrient for human health, particularly skin health, and biotin deficiency is associated with severe dermatologic conditions, including hair loss (Mock, 1991). Biotin deficiency can be induced by various factors, including polymorphisms in the biotinidase gene resulting in biotinidase deficiency (Wolf, 2012), long-term treatment with certain anticonvulsants (Krause et al., 1984; Mock and Dyken, 1997), intestinal malabsorption disorders (Khalidi et al., 1984), inflammatory bowel diseases, such as ulcerative colitis and Crohn's disease (Fernandez-Banares et al., 1989; Urabe, 1986), and consumption of excessive raw egg white (Mock et al., 2004). Pregnant women tend to be slightly biotin deficient despite normal dietary biotin intake (Mock and Stadler, 1997; Mock et al., 1997), and biotin deficiency is also relatively common in infants (Wolf, 2010). Because mammals lack the enzymes required to synthesize biotin, their required biotin levels that are

physiologically essential for the host are regulated redundantly by their diet and microbiota.

In the present study, we showed that long-term treatment with the antibiotic vancomycin resulted in the accumulation of vancomycin-resistant *L. murinus* in the intestine. Because this bacterium lacks the ability to produce biotin, a predominance of *L. murinus* concomitant with a lack of dietary biotin led to the development of a skin disease resembling alopecia in mice. This study thus demonstrates that gut dysbiosis promotes alopecia via biotin depletion in the gut and provides a basis for understanding the previously unknown link between gut microbiota and skin diseases.

## RESULTS

### Gut Dysbiosis Drives Alopecia

Recent studies indicate an association between dysbiosis in the gut and skin diseases, such as psoriasis and atopic dermatitis (Penders et al., 2007; Scher et al., 2015; Song et al., 2016). Biotin-deficient germ-free (GF) mice develop alopecia, which does not occur in conventional mice, suggesting that microbiota plays a pivotal role in biotin metabolism. To determine how gut bacterial dysbiosis contributes to alopecia, C57BL/6 wild-type (WT) mice were treated with antibiotics targeting gram-positive (vancomycin) and gram-negative (polymyxin B) bacteria and fed a diet with or without biotin (Figure 1A). None of the mice fed a biotin-deficient diet exhibited growth defects. Control mice exposed to dietary biotin deprivation did not show any signs of alopecia, however, mice developed alopecia when treated with vancomycin (Figure 1B). By contrast, no noticeable alopecia was observed in mice treated with polymyxin B (Figure 1B). Histological study detected an increase in anagen hair follicles in alopecic mice, which was not detected in the other groups (Figure 1C). However, detailed microscopic investigation of the skin surface revealed the breakage of hair shafts (Figure 1D), demonstrating that increased hair fragility in a hair shaft is a major contributing factor explaining the hair loss phenotype in alopecic mice. In addition, the expression of some inflammatory mediators in the skin was not increased in alopecic mice, although it remains possible that other, yet to be tested, inflammatory mediators are elevated in these mice (Figures 1E and S1). Hair loss appeared in the back in mice fed the biotin-deficient diet and treated with vancomycin for 4 weeks (Figure 1F). To assess the relation between alopecia and biotin production, biotin concentration was measured in the gut and serum. Affected mice showed a significant reduction of biotin levels in both the intestine and serum (Figures 1G and 1H).

### Mice with Alopecia Show Altered Gut Microbiota Composition

To characterize the microbiota composition in the colon, fecal samples from each mouse were analyzed by sequencing the 16S rRNA gene V3–V4 regions. From these samples, a total of 1,395,974 high quality 16S rRNA gene sequences were identified. The mean number of sequences obtained per sample was 48,137 (range: 30,906–71,595). Vancomycin treatment in mice with alopecia resulted in dramatic increases in Firmicutes phylum, especially *Lactobacillaceae* compared with the other groups in the gut (Figures 2A and S2). Principal-coordinates analysis (PCoA) plots of weighted UniFrac distances revealed that the gut microbiota profile of these alopecia mice was significantly distinct from that of the other groups (Figure 2B). Vancomycin, but not polymixin B, treatment significantly reduced bacterial diversity in both normal diet- and biotin (−) diet-fed groups compared to normal (normal diet and no antibiotics treated) control mice (Figure 2C). Alopecia mice (biotin [−] diet +VCM) showed further reduction of bacterial diversity compared to normal + VCM mice (normal diet and VCM) (Figure 2C). To identify a species level of the *Lactobacillus*, we performed phylogenetic analysis of the 16S rRNA gene sequence of isolated colonies from MRS (De Man, Rogosa and Sharpe) agar and compared the results with reference sequences obtained from the GenBank database. The strain was identified as *L. murinus* (Figure S3). qPCR analysis revealed that *Lactobacillus* genus and *Lactobacillus murinus* (*L. murinus*) species were significantly increased in alopecia mice (Figures 2D and 2E), however, total bacterial number was not significantly changed across groups (data not shown). These results indicated that gut dysbiosis accompanied with the domination of *L. murinus* might influence alopecia symptom.

### Alopecia Induced by Monocolonization of *L. murinus* in GF Mice Is Biotin Dependent

To determine whether the single strain of *L. murinus* plays a causal role in the induction of alopecia, GF mice were monocolonized with *L. murinus* isolated from feces of alopecia mice. Control GF mice and *L. murinus* monocolonized mice were then fed a biotin-deficient diet (Figure 3A). Scanning electron microscopy showed that *L. murinus* successfully colonized the proximal colon (Figure 3B). Consistent with previous reports, the gut microbiota plays a key role in the maintenance of biotin levels, as demonstrated in GF mice fed a biotin-deficient diet, which exhibits alopecia (Ikeda et al., 1996), deprivation of dietary biotin promoted the development of mild alopecia in GF mice (Figure 3C). Monocolonization of *L. murinus* further aggravated the alopecia symptom in GF mice fed a biotin-deficient diet (Figures 3C and 3D). However, GF mice fed a normal diet monocolonized with *L. murinus* did not show alopecia symptom (Figure S4). Most of the hair follicles in GF mice consuming a normal diet and GF mice fed a biotin-deficient diet were in the telogen phase, whereas the hair follicles of GF mice fed a biotin-deficient diet with *L.murinus* were in the proliferating anagen phase (Figure 3E). Consistent with data obtained from specific pathogen-free (SPF) mice (Figure 1C), cellular infiltration was not evident around hair follicles in all groups (Figure 3E). Furthermore, the expression of proinflammatory cytokine genes, such as tumor necrosis factor-$\alpha$ and interferon-$\gamma$ in the skin did not differ between the groups (Figure 3F). Biotin concentration both in the gut and serum was significantly decreased in the biotin-deficient group and was even lower in the biotin-deficient with *L. murinus* group (Figures 3G and 3H). This suggested that the consumption of residual luminal biotin by *L. murinus* in mice fed a biotin-deficient diet promotes the development of alopecia by depriving the host of biotin. In addition, capillary electrophoresis time-of-flight mass spectrometry (CE-TOFMS)-based metabolome analysis of serum samples followed by principal-component analysis (PCA) and hierarchical cluster analysis

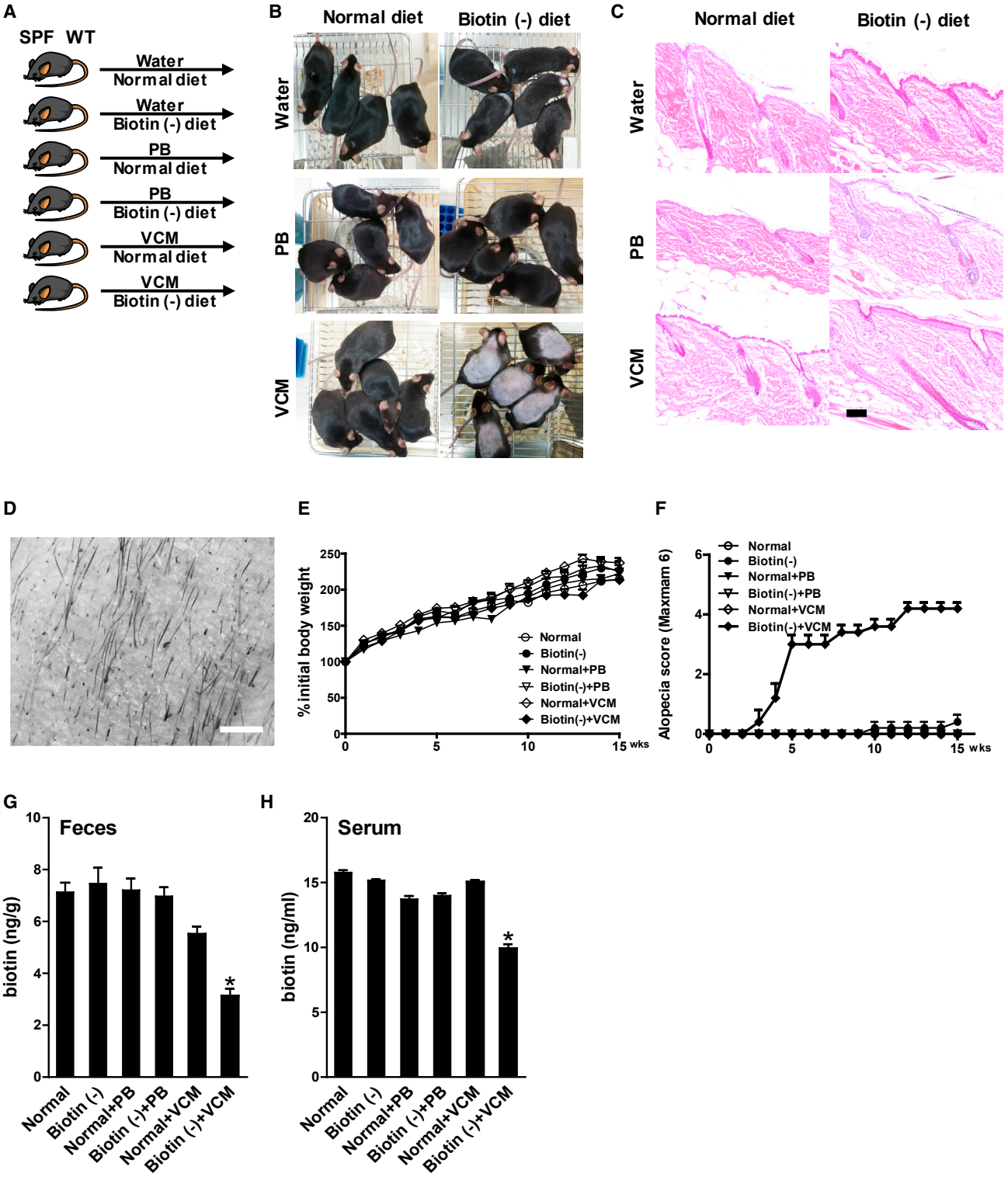


**Figure 1. Gut Dysbiosis Drives Alopecia**

(A) SPF mice were fed a normal diet or a diet excluding biotin and were divided into six groups and treated with water, polymyxin B, or vancomycin for 15 weeks.

(B) Example of antibiotic-induced alopecia in WT mice.

(C) Histopathology of the skin; original magnification. Scale bar, 100 μm. Approximately 30 hair follicles per mouse were analyzed, and H&E images are representative of each group.

*(legend continued on next page)*

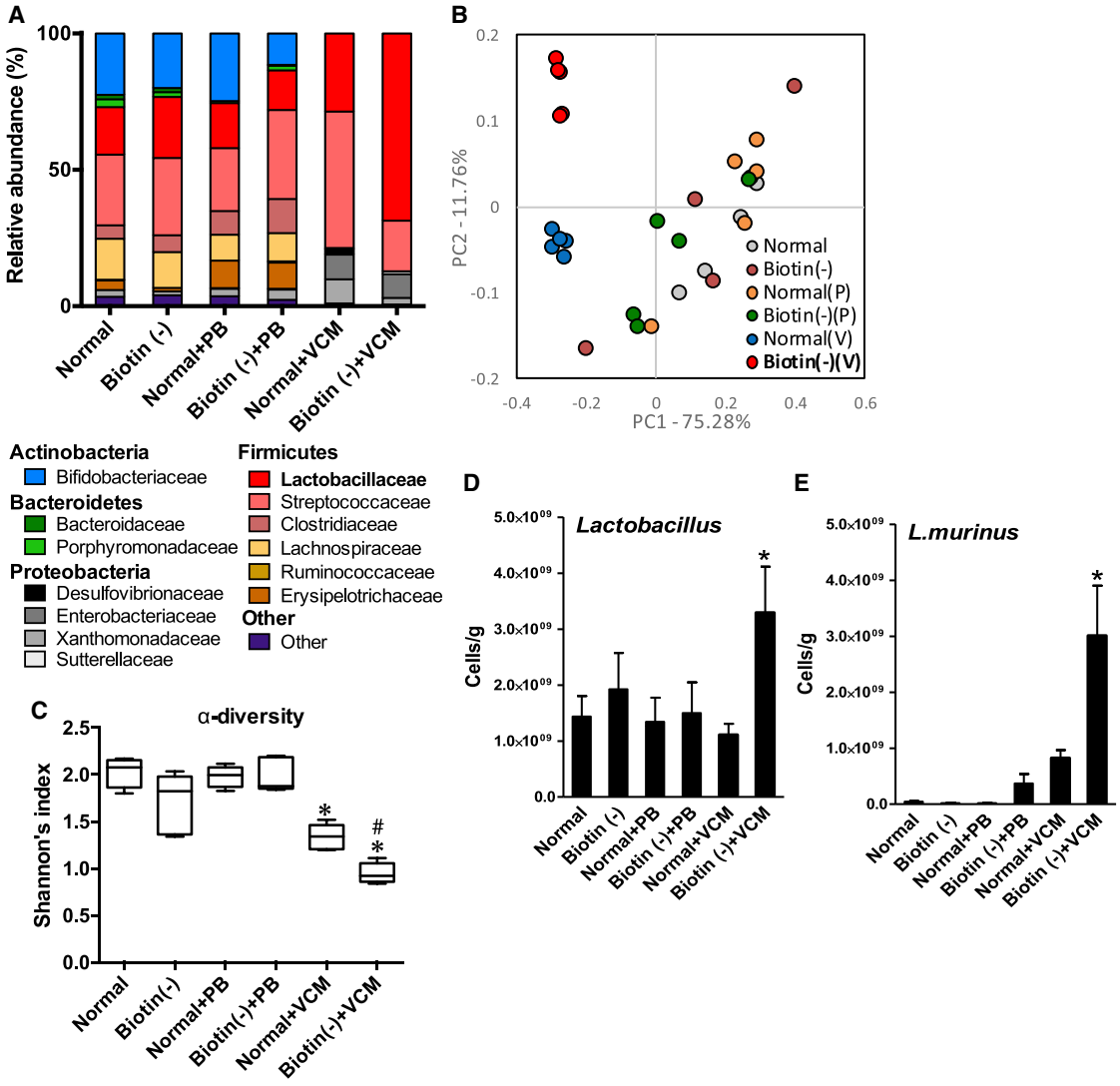


**Figure 2. Mice with Alopecia Show Altered Gut Microbiota Composition**

(A) The microbiota composition in feces was determined by 16S rRNA analysis. Taxon-based analysis at the family level among the groups is shown. The data are expressed as the percent relative abundance. See also Figure S2.

(B) The PCoA plots show six groups of subjects defined by weighted UniFrac microbiota analysis.

(C) Difference in Shannon-Wiener diversity among the different groups.

(D and E) Bacterial DNA from feces in each group of mice (D and E) was extracted and analyzed by qPCR for the 16S rRNA coding gene. Statistical data are expressed as the mean ± SEM (n = 4–5/group). The data were compared to normal mice as control (*$p < 0.05$). The data were compared to normal + VCM mice with biotin (−) + VCM mice ($^{\#}p < 0.05$). PB, polymyxin B. VCM, vancomycin.

See also Figures S2 and S3.

(HCA) showed that alopecia mice fed the biotin-deficient diet with *L. murinus* were distinct from other groups (Figures S5A–S5C). Notably, amino acids or fatty acid, such as 3-hydroxybutyrate enriched in alopecic mice were considered to be association biotin-dependent carboxylases (Figure S6; Table S2). Since patients with carboxylase deficiency are known to exhibit alopecia (Charles et al., 1979), alopecia induced by biotin deficiency presumably results from impaired activity of carboxylases.

(D) Microscopy of the skin; original magnification. Scale bar, 1 mm.

(E) Change in body weight.

(F) Alopecia was scored visually every week according to a 0–6 scoring system (Table S1).

(G and H) Biotin concentration was measured in feces (G) and serum (H) using a biotin assay. Statistical data are expressed as the mean ± SEM (n = 4–5/group). The data were compared to normal mice as control (*$p < 0.05$). PB, polymyxin B. VCM, vancomycin.

See also Figure S1.

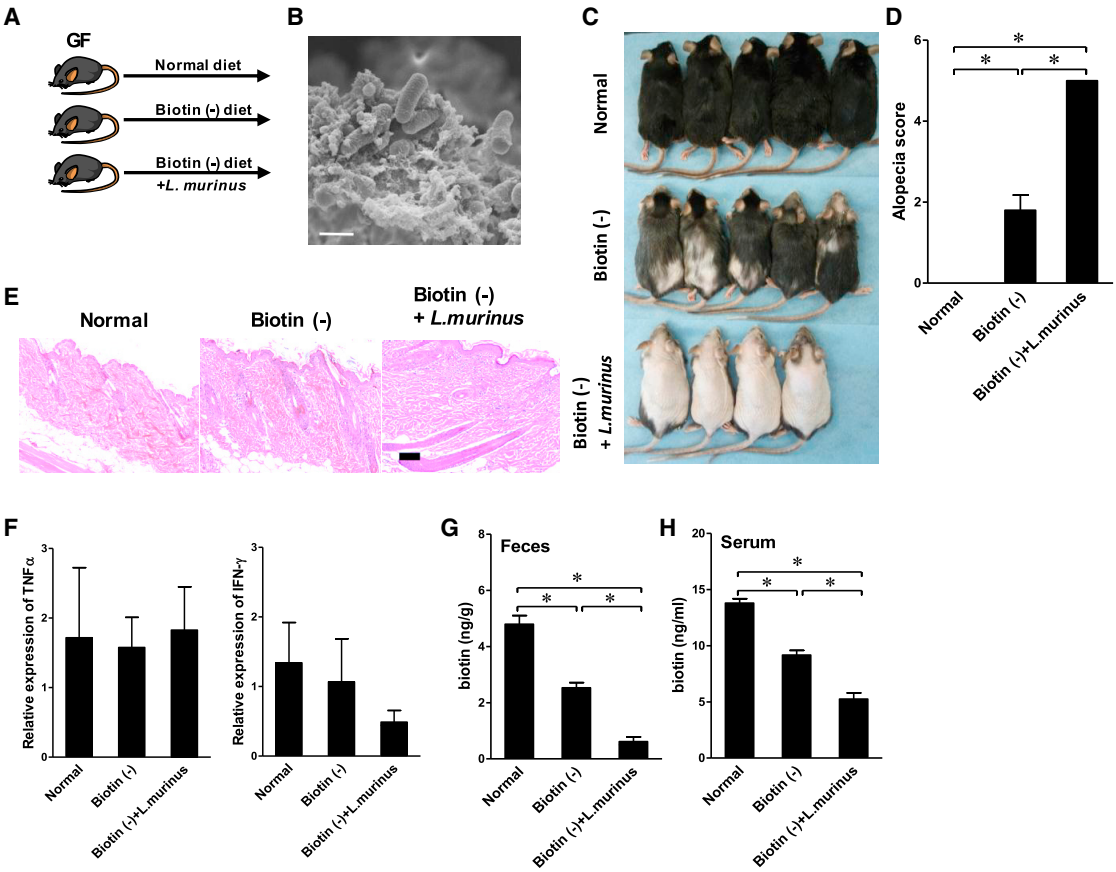


**Figure 3. Alopecia Induced by Monocolonization of *L. murinus* in GF Mice Is Biotin Dependent**

(A) Experimental design. GF mice were fed a normal diet until 4 weeks old. Then, these mice were fed a normal diet or a diet excluding biotin for 8 weeks. GF mice were either untreated or orally inoculated with *L.murinus* ($1 \times 10^8$ cells/200 μL).

(B) Scanning electron microscopy showing the distal colon of *L.murinus*-monoassociated mice fed a biotin-deficient diet. Scale bar, 1 μm.

(C) Example of alopecia.

(D) Alopecia was scored visually according to a 0–6 scoring system.

(E) Histopathology of the skin; original magnification. Scale bar, 100 μm.

(F) Expression of the indicated mRNAs in skin cells, normalized to Act-b expression.

(G and H) Biotin concentration was measured in feces (G) and serum (H) using a biotin assay. Statistical data are expressed as the mean ± SEM (n = 4–5/group). *$p < 0.05$. NS, not significant.

See also Figures S4–S6 and Table S2.

## Reinduction of Hair Growth by Supplementation of Biotin

We determined the extent to which complementation of biotin reverses alopecia symptoms in mice with concomitant biotin deficiency and gut dysbiosis. As described above, biotin deprivation with vancomycin-induced gut dysbiosis led to the development of severe alopecia. After the development of hair loss, one-half of the mice were returned to a normal diet, while the other half were maintained on a biotin-deficient diet with vancomycin. Biotin supplementation with cessation of vancomycin reversed the established alopecia symptoms (Figures 4A and 4B). To characterize the microbiota composition in the colon, samples from each mouse were analyzed by sequencing the 16S rRNA gene V3–V4 regions. From these samples, a total of 196,506 high quality 16S rRNA gene sequences were identified. The mean number of sequences obtained per sample was 24,563 (range: 9,926–48,700). The dominance of *Lactobacillaceae* in the biotin resupplementation group from feces was dramatically reduced (average: 57% versus 24%) compared with that in normal WT mice (Figures 4C and 4D). PCoA plots of weighted UniFrac distances showed that the gut microbiota profile of alopecia mice was significantly distinct from those of the other groups (Figure 4E). The diversity of the fecal gut microbiota of reversed alopecia mice was considerably greater than that of alopecia mice (Figure 4F). qPCR analysis revealed that *Lactobacillus* and *L. murinus* were significantly decreased in reversed alopecia mice (Figures 4G and 4H). These results suggested that alopecia was induced by gut dysbiosis, in particular the overgrowth of *L. murinus* and the consequent depletion of biotin. We next investigated the presence of genes related to biotin metabolism in this bacterium by examining the Kyoto Encyclopedia of Genes and Genomes (KEGG) pathway genes database

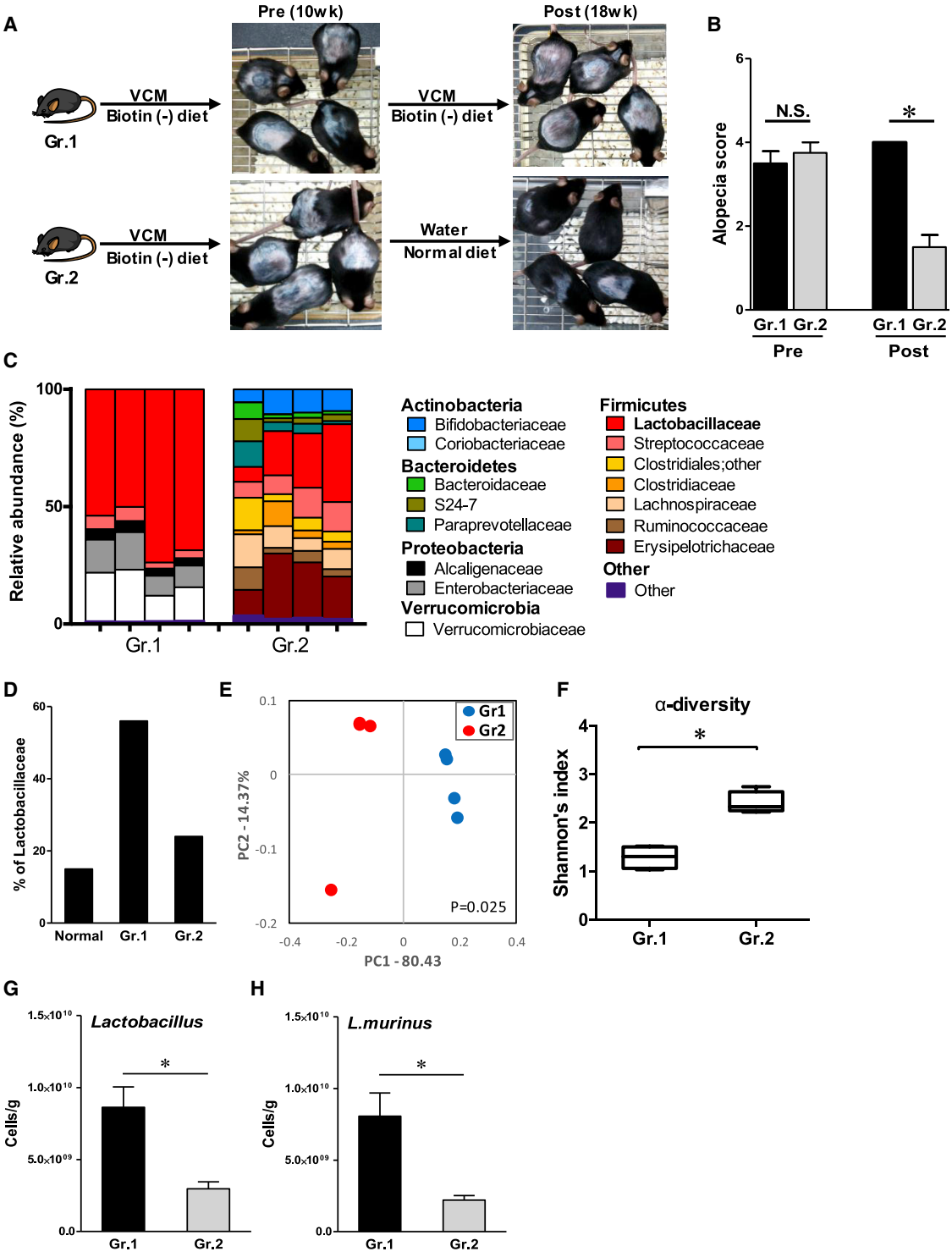


**Figure 4. Reinduction of Hair Growth by Supplementation of Biotin**

(A) Hair loss was induced in mice by feeding a diet excluding biotin and treatment with vancomycin for 10 weeks. Hair-loss mice were divided into two groups and fed a diet excluding biotin with vancomycin or a normal diet with water.

(B) Alopecia was scored visually according to a 0–6 scoring system.

(C) Microbiota composition of feces was determined by 16S rRNA analysis. Taxon-based analysis at family level among the groups is shown. The data are expressed as the percent relative abundance.

(D) The percent relative abundance of *Lactobacillaceae* from feces was determined by 16S rRNA analysis.

*(legend continued on next page)*

(Kanehisa and Goto, 2000). The *L. murinus* strain, which is dominated in the gut microbiota of alopecia mice, does not harbor biotin biosynthesis-related genes (*BioA*, *BioD*, and *BioC*) (Figures S7A and S7B). Thus, it is plausible that the domination of *L. murinus* affects the biosynthesis of biotin, thereby leading to biotin deficiency. Furthermore, the *L. murinus* strain, which accumulated in alopecia mice, reduced biotin concentration in vitro (Figure S7C). Since this *L. murinus* strain is unable to synthesize biotin, the domination of this *L. murinus* strain in the gut might reduce in vivo biotin availability.

### Systemic Biotin Treatment Restored Hair Growth via Microbiota Independent Pathway

To clarify the direct effect of biotin on alopecia, we performed systemic supplementation of biotin to alopecic mice. Intraperitoneal injection with biotin restored the serum biotin level and hair growth (Figures 5A, 5B, and 5D). Biotin concentration in feces was not restored by systemic biotin supplementation (Figure 5C), suggesting that serum, but not intestine biotin, level is important in maintaining normal hair growth. 16S rRNA gene sequences revealed the dominance of *Lactobacillaceae* in the gut was not significantly altered after systemic supplementation of biotin (Figure 5E). Normal and alopecic mice differ significantly in gut and skin microbiota, but alpha diversity of the gut microbiota was not significantly altered after treatment of biotin (Figures 5F and 5G). Taken together, biotin supplementation bypasses microbial dysbiosis and rescues hair physiology.

## DISCUSSION

The gut microbiota impacts on the pathophysiology of extra-intestinal tissues, including the skin. Here, we demonstrated that gut dysbiosis, induced by treatment with certain antibiotics, impaired biotin biosynthesis by the gut microbiota. Although reduced biotin synthesis by the gut microbiota was not immediately pathogenic if biotin was supplemented from dietary sources, lack of dietary biotin in antibiotic-treated, dysbiotic mice led to systemic biotin deficiency, resulting in the development of alopecia.

Gut microbiota synthesizes and supplies many essential B-group vitamins, including biotin (Hill, 1997; Singh et al., 2014). *Bacteroides spp.* overexpress the genes encoding four enzymes in the biotin-biosynthesis pathway (COG0132, COG0156, COG0161, and COG0502) (Arumugam et al., 2011; Sugahara et al., 2015), while other commensal bacteria, such as the *Lactobacillus* species, lack these biotin-synthesis genes and therefore fail to generate biotin. Notably, despite the inability to synthesize biotin, these bacteria can consume biotin supplied from the diet and/or from other bacteria such as *Bacteroides*. The balance between biotin-producing and -consuming bacteria thus controls the amount of luminal biotin available to the host. In the current study, we identified *L. murinus* in mice with biotin deficiency-induced alopecia as an "obligate biotin reducer". Although *L. murinus* lacks biotin-synthesis genes and therefore fails to generate biotin, it may nevertheless utilize biotin for its own growth. Indeed, the strain of *L. murinus* that we have isolated from alopecia mice can consume biotin for its growth in vitro, although in vitro reduction of biotin might not resemble the ecology of this bacterium in vivo. Mice deprived of external sources of biotin exhibit substantial amounts of fecal biotin because these mice can still utilize biotinylated proteins as a reservoir for biotin and secrete biotin into the gut and urine. Domination of *L. murinus* as a result of vancomycin treatment thus reduced the availability of luminal biotin, which in turn perturbed the biotin-recycling system in the gut and affected its systemic availability, with consequent impacts on skin physiology. Vancomycin-treated mice, which did not develop alopecia, exhibit a slight decrease of biotin in feces, but maintain a serum biotin level. These data indicate that the serum biotin level reflects alopecia symptoms. Importantly, supplementation of biotin via a systemic route bypassed the dysbiosis-induced decreased bioavailability of biotin in the gut and restored hair growth. These results demonstrate that physiological levels of systemic (and skin) biotin are regulated by the gut microbiota and dietary supplementation, and gut dysbiosis, as well as malnutrition, can thus disrupt skin physiology.

Hair loss can also be caused by various disorders, such as hormone changes, malnutrition, and as a side effect of medication. The pathogeneses of these diseases are tightly linked to the hair-growth cycle (Shrivastava, 2009). The normal hair cycle consists of three distinct stages: anagen (active hair growth), catagen (involution), and telogen (resting) phase. During normal hair-growth cycles in humans, hair on the scalp is replaced every 3–5 years, and scalp follicles give rise to 10–30 cycles in a lifetime (Harrison and Sinclair, 2002; Kligman, 1959), while the equivalent hair-follicle cycle in C57BL/6 mice lasts 4–6 weeks (Müller-Röver et al., 2001). Telogen effluvium occurs when a large number of hair follicles enter telogen (Malkud, 2015). The hair follicles remain intact and undergo spontaneous anagen, resulting in normal hair regeneration in most patients with acute telogen effluvium (Malkud, 2015). In contrast, anagen effluvium is induced in patients undergoing chemotherapy (Yun and Kim, 2007). Chemotherapy is thought to attack hair follicles, leading to hair fragility. Disruption of the normal hair-growth cycle and abnormal hair fragility lead to excessive shedding of hair and consequent alopecia.

Although biotin deficiency is known to cause hair loss (Zempleni et al., 2008), the precise mechanism responsible for the alopecic symptoms remains unclear. However, biotin was shown to play a role in keratinocyte proliferation and differentiation in HaCaT cells (Grafe et al., 2003). Biotin deficiency-induced alopecia is considered to represent a failure of hair retention caused by faulty keratinization of the hair shaft (Rauch, 1952), suggesting that the hair shaft breaks off easily, distal to the club. Consistent with these observations, the results of the current study indicated that hair follicles were retained and in

(E) The PCoA plots show two groups of subjects defined by weighted UniFrac microbiota analysis.
(F) Difference in Shannon-Wiener diversity among the different groups.
(G and H) Bacterial DNA from the feces in each group of mice (G and H) was extracted and analyzed by qPCR for the 16S rRNA coding gene. Statistical data are expressed as the mean ± SEM (n = 4/group). *p < 0.05. NS, not significant.
See also Figure S7.

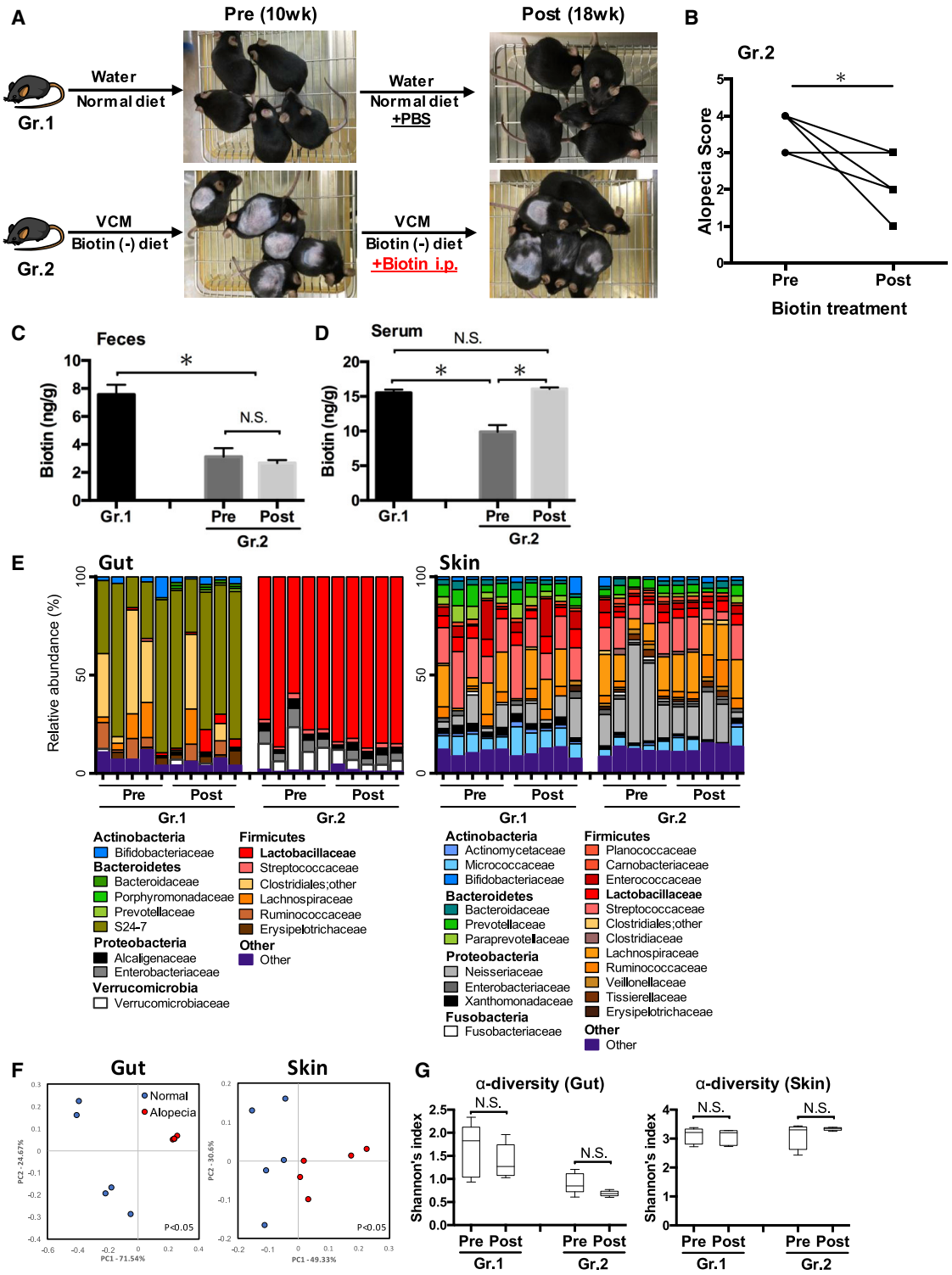


**Figure 5. Systemic Biotin Treatment Restored Hair Growth via Microbiota-Independent Pathway**

(A–D) Experimental design and example of alopecia. SPF mice were fed a normal diet or a diet excluding biotin and treated with water or vancomycin for 10 weeks (pre). Then, normal mice were intraperitoneally injected with PBS (gr.1) or alopecic mice were injected with biotin (100 μg/100 μL) (gr. 2) every other day for 8 weeks (post) (A). Alopecia score (B) and fecal (C) and serum (D) biotin concentration were measured.

*(legend continued on next page)*

proliferating anagen phase in mice with biotin deficiency-induced alopecia. Microscopic examination showed a "black dot" sign in the alopecic lesion, indicating the broken hair shaft and suggesting that the hair shaft was fragile in these mice.

Biotin serves as a co-factor for multiple carboxylases, such as methylcrotonyl-coenzyme A (CoA) carboxylase, pyruvate carboxylase, acetyl-CoA carboxylase, and propionyl-CoA carboxylase (Zempleni et al., 2012). Biotinylation of these enzymes is catalyzed by holocarboxylase synthetase (Donti et al., 2016; Pérez-Monjaras et al., 2008). Similar to biotin-deficiency alopecia in humans, patients with defects in single or multiple carboxylases also exhibit alopecia (Burri et al., 1981; Charles et al., 1979; Munnich et al., 1980). Biotin clearly contributes to the metabolism of amino acids and lipids by several carboxylases, and biotin deficiency thus results in significant alterations in the systemic metabolic profile. Animals fed a biotin-deficient diet showed higher levels of branched-chain amino acids (isoleucine, leucine, and valine) than those fed a normal diet, suggesting that normal amino acid metabolism is perturbed by a biotin-deficient diet, and that this metabolic alteration may be exacerbated by *L. murinus*. We also detected the accumulation of organic acids, such as 3-hydroxybutyrate, in biotin-deficient mice, similar to the situation reported in patients with carboxylase deficiencies (Baumgartner and Suormala, 1997; Schürmann et al., 1997). These data imply that hair fragility in biotin-deficient mice is likely to be caused by a failure of the normal metabolism of amino acids or their intermediate metabolites.

Similar to the close relationship between resident microbes and the immune system in the gut, the resident skin microbiota regulates immune development/activation in the skin (Belkaid and Tamoutounour, 2016; Naik et al., 2012; Grice et al., 2009). Perturbation of the skin microbiota may thus have significant influences on disease pathogenesis in the skin, such as in the development of atopic dermatitis (Kobayashi et al., 2015; Kong et al., 2012; Leyden et al., 1974). In the present study, PCoA of skin microbiota is significantly different between normal and alopecic mice. Therefore, it is still possible that dysbiotic microbiota in the skin is enriched by bacteria that over consume biotin and might be sufficient to induce alopecia independent of gut dysbiosis. The role of skin microbiota in the development of alopecia caused by biotin deficiency continues to remain to be elusive.

In conclusion, we demonstrated that the gut microbiota plays a role in the pathogenesis of alopecia. Gut dysbiosis, especially overgrowth of *L. murinus*, and subsequent biotin deficiency are critical steps leading to the development of alopecia. The gut microbiota and its metabolism are thus potential targets for the management of skin diseases with impaired hair physiology.

## EXPERIMENTAL PROCEDURES

### Animals

C57BL/6 mice were purchased from Japan Clea (Tokyo, Japan). GF C57BL/6 mice were purchased from Sankyo Laboratories (Tokyo, Japan). GF and gnotobiotic mice were maintained in vinyl isolators within the gnotobiotic facility of the Miyarisan Pharmaceutical (Nagano, Japan). Other mice were maintained under SPF conditions in the Animal Care Facility of Keio University. Male mice at the age of 4–6 weeks were used in all experiments. All experiments were approved by the regional animal study committees and were performed according to institutional guidelines. Experimental diets both AIN93G (normal) and AIN93G without biotin (biotin deficient) were purchased from Oriental Yeast. Diet composition data shown in Table S3.

### Fecal DNA Extraction for Meta 16S rRNA Gene Sequencing

The fecal contents from mice were immediately frozen in liquid nitrogen and stored at −80°C until use. Fecal pellets were suspended in 10 mM Tris-HCl and 10 mM EDTA buffer (pH 8.0) and incubated with lysozyme (Sigma, final concentration: 15 mg/mL) at 37°C for 1 hr. A purified achromopeptidase (Wako) was added (final concentration: 2,000 U/mL) and further incubated at 37°C for another 30 min. Then, SDS (final concentration: 1%) was added to the cell suspension and mixed well. Subsequently, proteinase K (Merck) was added (final concentration: 1 mg/mL) to the suspension, and the mixture was incubated at 55°C for 1 hr. High-molecular-mass DNA was isolated and purified by phenol/chloroform extraction, ethanol, and finally polyethylene glycol precipitation.

### Skin Microbiome DNA Extraction for Meta 16S rRNA Gene Sequencing

Skin microbiota was collected with a swab (BD) moistened with 1.2% Triton X-100 and 20 mM Tris-EDTA microbiome DNA was extracted using PureLink Microbiome DNA Purification Kit (Invitrogen), according to the manufacture's instruction.

### Sequence Analysis Pipeline

The 16S rRNA sequence data generated by the MiSeq sequencer (Illumina) were processed by the quantitative insights into microbial ecology (QIIME 1.8.0) pipeline (Caporaso et al., 2010a, 2010b). Sequences with an average quality value of <20 were filtered out. Chimeric sequences were removed using USEARCH (Edgar, 2010). Sequences were clustered into operational taxonomic units (OTUs) based on 97% sequence similarity at the species level using UCLUST (Edgar, 2010) against Greengenes database 13_8 (DeSantis et al., 2006). A representative sequence for each OTU was aligned with PyNAST (Caporaso et al., 2010a). Bacterial taxonomy was assigned using UCLUST (Edgar, 2010). Genomic DNA from Microbial Mock Community B (BEI Resources) was used in the study to evaluate data analysis procedures. Diversity analyses were used QIIME script *core_diversity_analyses.py*. Microbiota diversity was measured by the Shannon index. Statistical significance of sample groupings was assessed using permutational multivariate ANOVA (PERMANOVA) (QIIME script *compare_categories.py*).

### Meta 16S rRNA Gene Sequencing

PCR was performed using Ex Taq Hot Start (TAKARA) and the Illumina forward primer 5′-AATGATACGGCGACCACCGAGATCTACAC (adaptor sequence) + barcode (eight bases) + ACACTCTTTCCCTACACGACGCTCTTCCGATCT (sequence primer) + CCTACGGGNGGCWGCAG-3′ (341F) and the Illumina reverse primer 5′-CAAGCAGAAGACGGCATACGAGAT (adaptor sequence) + barcode (eight bases) + GTGACTGGAGTTCAGACGTGTGCTCTTCCGATCT (sequence primer) + GACTACHVGGGTATCTAATCC-3′ (805R) to the hypervariable V3–V4 region of the 16Sr RNA gene. Amplicons generated from each sample were subsequently purified using AMPure XP (Beckman Coulter). The amount of DNA was quantified using a Quantus Fluorometer and the QuantiFluor dsDNA System (Promega). Mixed samples were prepared by pooling approximately equal amounts of each amplified DNA and sequenced

(E) The microbiota composition in feces and skin from the mice were determined by 16S rRNA analysis. Taxon-based analysis at the family level among the groups is shown. The data are expressed as the percent relative abundance.
(F) PCoA plots in gut and skin show two groups of subjects defined by weighted UniFrac microbiota analysis.
(G) Difference in Shannon-Wiener diversity among the groups. Statistical data are expressed as the mean ± SEM (n = 5/group). *p < 0.05. NS, not significant.

using MiSeq Reagent Kit V3 (600 cycle) and MiSeq sequencer (Illumina), according to the manufacturer's instructions.

### Isolation of Bacterial Strains

*L. murinus* was isolated from fecal samples that were aseptically spread on MRS agar (BD Difco) for isolating lactobacilli. The strain was cultured in an anaerobic jar at 37°C for 48 hr. Several colonies were suspended in 1 mL of TE buffer (10 mM Tris-HCl and 1 mM EDTA [pH 8.0]) and boiled for 10 min. After centrifugation at 9,000 *g* for 1 min, the supernatants were used as templates for PCR amplification. Amplification was performed in a 50 μL reaction mixture containing 1 × Ex Taq buffer, 0.2 mM of each dNTP, 1.25 units of Ex Taq HS (Takara), 10 pmol of each forward primer 5′-AGAGTTTGATCCTGGCTCAG-3′ and reverse primer 5′-GGTTACCTTGTTACGACTT-3′, and 1 μL of template. After preincubation at 95°C for 3 min, 30 cycles consisting of 95°C for 30 s, annealing at 55°C for 30 s, and extension at 72°C for 1.5 min were performed, followed by a final extension step of 5 min at 72°C. PCR amplicons were purified using AMPure XP. The 16S rRNA was sequenced using BigDye Terminator v3.1 Cycle Sequencing Kit and ABI PRISM 3130 Genetic Analyzer (Applied Biosystems). Reference sequences were obtained from the GenBank database and aligned using the multisequence alignment program ClustalW (Thompson et al., 1994). Phylogenetic relationships among the individual sequence types were determined using the neighbor-joining algorithm of molecular evolutionary genetics analysis (MEGA) v.6 (Tamura et al., 2013).

### Biotin Bioassay

Biotin concentration was measured from serum and feces, as described previously with modifications. Briefly, *Lactobacillus plantarum* American Type Culture Collection (ATCC) 8014 was cultured at 37°C for 15–20 hr in MRS broth (BD Difco). The cells were washed twice with distilled water and suspended in distilled water. Biotin Assay Medium (Nissui) was autoclaved at 121°C for 5 min. The bacterial suspension was inoculated into the Biotin Assay Medium at a concentration of 1 μg/mL. To generate standards, D-biotin (Sigma) was dissolved in 50% ethanol to 100 μg/mL and diluted with 95% ethanol to a concentration of 1 μg/mL. The standard biotin solution was diluted with distilled water to a final concentration ranging from 2.0 to 0.125 ng/mL. A volume equal to 100 μL of sample or standard was inoculated into 900 μL of Biotin Assay Medium and incubated at 37°C for 16–20 hr. The absorbance was measured at 600 nm.

### Statistical Analysis

The results were expressed as the mean ± SEM. Data were analyzed with GraphPad Prism statistical software using ANOVA followed by a Mann-Whitney test, Dunnett's multiple comparison test, and Bonferroni test. Microbiota diversity was estimated by Shannon index. PERMANOVA was used with 999 permutation to the weighted UniFrac distance matrix. Differences were considered to be statistically significant when $p < 0.05$.

## ACCESSION NUMBERS

The accession number for the 16S rRNA sequence of *L. murinus* reported in this paper is DDBJ: LC159538. The accession number for the genome sequence of *L. murinus* reported in this paper is DDBJ: BDFM01000001-BDFM01000358.

## SUPPLEMENTAL INFORMATION

Supplemental Information includes Supplemental Experimental Procedures, seven figures, and three tables and can be found with this article online at http://dx.doi.org/10.1016/j.celrep.2017.07.057.

## AUTHOR CONTRIBUTIONS

Conceptualization, A.H., Y.M., and T.K.; Methodology, A.H., Y.M., K.M., R.A., T.T., and S.F.; Formal Analysis, A.H. and K.M.; Investigation, A.H., Y.M., K.M., S.F., and T.K.; Writing - Original Draft, A.H., Y.M., N.K., T.S., and T.K.; Writing - Review and Editing, A.H., Y.M., N.K., and T.K.; Visualization, A.H., Y.M., K.M., and S.F.; Project Administration, T.S., S.M., M.N., W.S., M.H., and M.A.; Supervision, M.O. and T.K.; and Funding Acquisition, T.K.

## ACKNOWLEDGMENTS

We thank Drs. Hiroki Kiyohara, Mari Arai, Makoto Mutaguchi, Keiko Ono, Takeru Amiya, Takahiro Suzuki, Moeko Nakashima (Keio University), Tetsuro Kobayashi, and Keisuke Nagao (NIH) for technical assistance. This study was supported in part by grants-in-aid for Scientific Research (15H02534), Scientific Research on Priority Areas, Exploratory Research, and Creative Scientific Research from the Japanese Ministry of Education, Culture, Sports, Science and Technology; the Japanese Ministry of Health, Labour and Welfare; Japan Agency for Medical Research and Development (AMED) (AMED-CREST; 16gm1010003h0001); Miyarisan Pharmaceutical Co., Ltd; Ezaki Glico Co., Ltd.; and the Keio University Medical Fund. A.H. and K.M. are supported by Miyarisan Pharmaceutical Co., Ltd. Y.M. is supported by research fellowships of Japan Society for the Promotion of Science. R.A. is supported by Ezaki Glico Co., Ltd.

Received: June 10, 2016
Revised: March 3, 2017
Accepted: July 19, 2017
Published: August 15, 2017

## REFERENCES

Arumugam, M., Raes, J., Pelletier, E., Le Paslier, D., Yamada, T., Mende, D.R., Fernandes, G.R., Tap, J., Bruls, T., Batto, J.M., et al.; MetaHIT Consortium (2011). Enterotypes of the human gut microbiome. Nature *473*, 174–180.

Atarashi, K., Tanoue, T., Oshima, K., Suda, W., Nagano, Y., Nishikawa, H., Fukuda, S., Saito, T., Narushima, S., Hase, K., et al. (2013). Treg induction by a rationally selected mixture of Clostridia strains from the human microbiota. Nature *500*, 232–236.

Baumgartner, E.R., and Suormala, T. (1997). Multiple carboxylase deficiency: inherited and acquired disorders of biotin metabolism. Int. J. Vitam. Nutr. Res. *67*, 377–384.

Belkaid, Y., and Tamoutounour, S. (2016). The influence of skin microorganisms on cutaneous immunity. Nat. Rev. Immunol. *16*, 353–366.

Burri, B.J., Sweetman, L., and Nyhan, W.L. (1981). Mutant holocarboxylase synthetase: evidence for the enzyme defect in early infantile biotin-responsive multiple carboxylase deficiency. J. Clin. Invest. *68*, 1491–1495.

Caporaso, J.G., Bittinger, K., Bushman, F.D., DeSantis, T.Z., Andersen, G.L., and Knight, R. (2010a). PyNAST: a flexible tool for aligning sequences to a template alignment. Bioinformatics *26*, 266–267.

Caporaso, J.G., Kuczynski, J., Stombaugh, J., Bittinger, K., Bushman, F.D., Costello, E.K., Fierer, N., Peña, A.G., Goodrich, J.K., Gordon, J.I., et al. (2010b). QIIME allows analysis of high-throughput community sequencing data. Nat. Methods *7*, 335–336.

Charles, B.M., Hosking, G., Green, A., Pollitt, R., Bartlett, K., and Taitz, L.S. (1979). Biotin-responsive alopecia and developmental regression. Lancet *2*, 118–120.

De Minicis, S., Rychlicki, C., Agostinelli, L., Saccomanno, S., Candelaresi, C., Trozzi, L., Mingarelli, E., Facinelli, B., Magi, G., Palmieri, C., et al. (2014). Dysbiosis contributes to fibrogenesis in the course of chronic liver injury in mice. Hepatology *59*, 1738–1749.

DeSantis, T.Z., Hugenholtz, P., Larsen, N., Rojas, M., Brodie, E.L., Keller, K., Huber, T., Dalevi, D., Hu, P., and Andersen, G.L. (2006). Greengenes, a chimera-checked 16S rRNA gene database and workbench compatible with ARB. Appl. Environ. Microbiol. *72*, 5069–5072.

Donti, T.R., Blackburn, P.R., and Atwal, P.S. (2016). Holocarboxylase synthetase deficiency pre and post newborn screening. Mol. Genet. Metab. Rep. *7*, 40–44.

Edgar, R.C. (2010). Search and clustering orders of magnitude faster than BLAST. Bioinformatics *26*, 2460–2461.

Fernandez-Banares, F., Abad-Lacruz, A., Xiol, X., Gine, J.J., Dolz, C., Cabre, E., Esteve, M., Gonzalez-Huix, F., and Gassull, M.A. (1989). Vitamin status in patients with inflammatory bowel disease. Am. J. Gastroenterol. *84*, 744–748.

Grafe, F., Wohlrab, W., Neubert, R.H., and Brandsch, M. (2003). Transport of biotin in human keratinocytes. J. Invest. Dermatol. *120*, 428–433.

Grice, E.A., Kong, H.H., Conlan, S., Deming, C.B., Davis, J., Young, A.C., Bouffard, G.G., Blakesley, R.W., Murray, P.R., Green, E.D., et al.; NISC Comparative Sequencing Program (2009). Topographical and temporal diversity of the human skin microbiome. Science *324*, 1190–1192.

Hand, T.W. (2016). The role of the microbiota in shaping infectious immunity. Trends Immunol. *37*, 647–658.

Harrison, S., and Sinclair, R. (2002). Telogen effluvium. Clin. Exp. Dermatol. *27*, 389–395.

Hill, M.J. (1997). Intestinal flora and endogenous vitamin synthesis. Eur. J. Cancer Prev. *6* (*Suppl 1*), S43–S45.

Ikeda, M., Uno, Y., Hamada, K., Kawabe, H., and Sakakibara, B. (1996). Effect of primary biotin deficiency on the skin of germ-free and conventional mice fed a purified biotin-deficient diet without supplementation with egg white. J. Clin. Biochem. Nutr. *22*, 63–72.

Ivanov, I.I., Frutos, Rde.L., Manel, N., Yoshinaga, K., Rifkin, D.B., Sartor, R.B., Finlay, B.B., and Littman, D.R. (2008). Specific microbiota direct the differentiation of IL-17-producing T-helper cells in the mucosa of the small intestine. Cell Host Microbe *4*, 337–349.

Kamada, N., and Núñez, G. (2013). Role of the gut microbiota in the development and function of lymphoid cells. J. Immunol. *190*, 1389–1395.

Kamada, N., Seo, S.U., Chen, G.Y., and Núñez, G. (2013). Role of the gut microbiota in immunity and inflammatory disease. Nat. Rev. Immunol. *13*, 321–335.

Kanehisa, M., and Goto, S. (2000). KEGG: kyoto encyclopedia of genes and genomes. Nucleic Acids Res. *28*, 27–30.

Kau, A.L., Ahern, P.P., Griffin, N.W., Goodman, A.L., and Gordon, J.I. (2011). Human nutrition, the gut microbiome and the immune system. Nature *474*, 327–336.

Khalidi, N., Wesley, J.R., Thoene, J.G., Whitehouse, W.M., Jr., and Baker, W.L. (1984). Biotin deficiency in a patient with short bowel syndrome during home parenteral nutrition. JPEN J. Parenter. Enteral Nutr. *8*, 311–314.

Kligman, A.M. (1959). The human hair cycle. J. Invest. Dermatol. *33*, 307–316.

Kobayashi, T., Glatz, M., Horiuchi, K., Kawasaki, H., Akiyama, H., Kaplan, D.H., Kong, H.H., Amagai, M., and Nagao, K. (2015). Dysbiosis and Staphylococcus aureus colonization drives inflammation in atopic dermatitis. Immunity *42*, 756–766.

Kong, H.H., Oh, J., Deming, C., Conlan, S., Grice, E.A., Beatson, M.A., Nomicos, E., Polley, E.C., Komarow, H.D., Murray, P.R., et al.; NISC Comparative Sequence Program (2012). Temporal shifts in the skin microbiome associated with disease flares and treatment in children with atopic dermatitis. Genome Res. *22*, 850–859.

Krause, K.H., Kochen, W., Berlit, P., and Bonjour, J.P. (1984). Excretion of organic acids associated with biotin deficiency in chronic anticonvulsant therapy. Int. J. Vitam. Nutr. Res. *54*, 217–222.

Lee, Y.K., Menezes, J.S., Umesaki, Y., and Mazmanian, S.K. (2011). Proinflammatory T-cell responses to gut microbiota promote experimental autoimmune encephalomyelitis. Proc. Natl. Acad. Sci. USA *108* (*Suppl 1*), 4615–4622.

Leyden, J.J., Marples, R.R., and Kligman, A.M. (1974). Staphylococcus aureus in the lesions of atopic dermatitis. Br. J. Dermatol. *90*, 525–530.

Malkud, S. (2015). Telogen effluvium: a review. J. Clin. Diagn. Res. *9*, WE01–WE03.

Mock, D.M. (1991). Skin manifestations of biotin deficiency. Semin. Dermatol. *10*, 296–302.

Mock, D.M., and Dyken, M.E. (1997). Biotin catabolism is accelerated in adults receiving long-term therapy with anticonvulsants. Neurology *49*, 1444–1447.

Mock, D.M., and Stadler, D.D. (1997). Conflicting indicators of biotin status from a cross-sectional study of normal pregnancy. J. Am. Coll. Nutr. *16*, 252–257.

Mock, D.M., Stadler, D.D., Stratton, S.L., and Mock, N.I. (1997). Biotin status assessed longitudinally in pregnant women. J. Nutr. *127*, 710–716.

Mock, D.M., Henrich-Shell, C.L., Carnell, N., Stumbo, P., and Mock, N.I. (2004). 3-Hydroxypropionic acid and methylcitric acid are not reliable indicators of marginal biotin deficiency in humans. J. Nutr. *134*, 317–320.

Müller-Röver, S., Handjiski, B., van der Veen, C., Eichmüller, S., Foitzik, K., McKay, I.A., Stenn, K.S., and Paus, R. (2001). A comprehensive guide for the accurate classification of murine hair follicles in distinct hair cycle stages. J. Invest. Dermatol. *117*, 3–15.

Munnich, A., Saudubray, J.M., Coude, F.X., Charpentier, C., Saurat, J.H., and Frezal, J. (1980). Fatty-acid-responsive alopecia in multiple carboxylase deficiency. Lancet *1*, 1080–1081.

Naik, S., Bouladoux, N., Wilhelm, C., Molloy, M.J., Salcedo, R., Kastenmuller, W., Deming, C., Quinones, M., Koo, L., Conlan, S., et al. (2012). Compartmentalized control of skin immunity by resident commensals. Science *337*, 1115–1119.

Olszak, T., An, D., Zeissig, S., Vera, M.P., Richter, J., Franke, A., Glickman, J.N., Siebert, R., Baron, R.M., Kasper, D.L., and Blumberg, R.S. (2012). Microbial exposure during early life has persistent effects on natural killer T cell function. Science *336*, 489–493.

Penders, J., Stobberingh, E.E., van den Brandt, P.A., and Thijs, C. (2007). The role of the intestinal microbiota in the development of atopic disorders. Allergy *62*, 1223–1236.

Pérez-Monjaras, A., Cervantes-Roldán, R., Meneses-Morales, I., Gravel, R.A., Reyes-Carmona, S., Solórzano-Vargas, S., González-Noriega, A., and León-Del-Río, A. (2008). Impaired biotinidase activity disrupts holocarboxylase synthetase expression in late onset multiple carboxylase deficiency. J. Biol. Chem. *283*, 34150–34158.

Rauch, H. (1952). The effects of biotin deficiency on hair development and pigmentation. Physiol. Zool. *25*, 145–149.

Said, H.M., and Mohammed, Z.M. (2006). Intestinal absorption of water-soluble vitamins: an update. Curr. Opin. Gastroenterol. *22*, 140–146.

Scher, J.U., Ubeda, C., Artacho, A., Attur, M., Isaac, S., Reddy, S.M., Marmon, S., Neimann, A., Brusca, S., Patel, T., et al. (2015). Decreased bacterial diversity characterizes the altered gut microbiota in patients with psoriatic arthritis, resembling dysbiosis in inflammatory bowel disease. Arthritis Rheumatol. *67*, 128–139.

Schürmann, M., Engelbrecht, V., Lohmeier, K., Lenard, H.G., Wendel, U., and Gärtner, J. (1997). Cerebral metabolic changes in biotinidase deficiency. J. Inherit. Metab. Dis. *20*, 755–760.

Shrivastava, S.B. (2009). Diffuse hair loss in an adult female: approach to diagnosis and management. Indian J. Dermatol. Venereol. Leprol. *75*, 20–27, quiz 27–28.

Singh, N., Gurav, A., Sivaprakasam, S., Brady, E., Padia, R., Shi, H., Thangaraju, M., Prasad, P.D., Manicassamy, S., Munn, D.H., et al. (2014). Activation of Gpr109a, receptor for niacin and the commensal metabolite butyrate, suppresses colonic inflammation and carcinogenesis. Immunity *40*, 128–139.

Sommer, F., and Bäckhed, F. (2013). The gut microbiota–masters of host development and physiology. Nat. Rev. Microbiol. *11*, 227–238.

Song, H., Yoo, Y., Hwang, J., Na, Y.C., and Kim, H.S. (2016). Faecalibacterium prausnitzii subspecies-level dysbiosis in the human gut microbiome underlying atopic dermatitis. J. Allergy Clin. Immunol. *137*, 852–860.

Sugahara, H., Odamaki, T., Fukuda, S., Kato, T., Xiao, J.Z., Abe, F., Kikuchi, J., and Ohno, H. (2015). Probiotic Bifidobacterium longum alters gut luminal metabolism through modification of the gut microbial community. Sci. Rep. *5*, 13548.

Tamura, K., Stecher, G., Peterson, D., Filipski, A., and Kumar, S. (2013). MEGA6: molecular evolutionary genetics analysis version 6.0. Mol. Biol. Evol. *30*, 2725–2729.

Thompson, J.D., Higgins, D.G., and Gibson, T.J. (1994). CLUSTAL W: improving the sensitivity of progressive multiple sequence alignment through sequence weighting, position-specific gap penalties and weight matrix choice. Nucleic Acids Res. *22*, 4673–4680.

Urabe, K. (1986). [Decreased plasma biotin levels in patients with Crohn's disease]. Nippon Shokakibyo Gakkai Zasshi *83*, 697.

Wolf, B. (2010). Clinical issues and frequent questions about biotinidase deficiency. Mol. Genet. Metab. *100*, 6–13.

Wolf, B. (2012). Biotinidase deficiency: "if you have to have an inherited metabolic disease, this is the one to have". Genet. Med. *14*, 565–575.

Yun, S.J., and Kim, S.J. (2007). Hair loss pattern due to chemotherapy-induced anagen effluvium: a cross-sectional observation. Dermatology (Basel) *215*, 36–40.

Zempleni, J., Hassan, Y.I., and Wijeratne, S.S. (2008). Biotin and biotinidase deficiency. Expert Rev. Endocrinol. Metab. *3*, 715–724.

Zempleni, J., Teixeira, D.C., Kuroishi, T., Cordonier, E.L., and Baier, S. (2012). Biotin requirements for DNA damage prevention. Mutat. Res. *733*, 58–60.

**Cell Reports, Volume *20***

## Supplemental Information

# Intestinal Dysbiosis and Biotin Deprivation Induce Alopecia through Overgrowth of *Lactobacillus murinus* in Mice

**Atsushi Hayashi, Yohei Mikami, Kentaro Miyamoto, Nobuhiko Kamada, Toshiro Sato, Shinta Mizuno, Makoto Naganuma, Toshiaki Teratani, Ryo Aoki, Shinji Fukuda, Wataru Suda, Masahira Hattori, Masayuki Amagai, Manabu Ohyama, and Takanori Kanai**

**Supplemental Information**

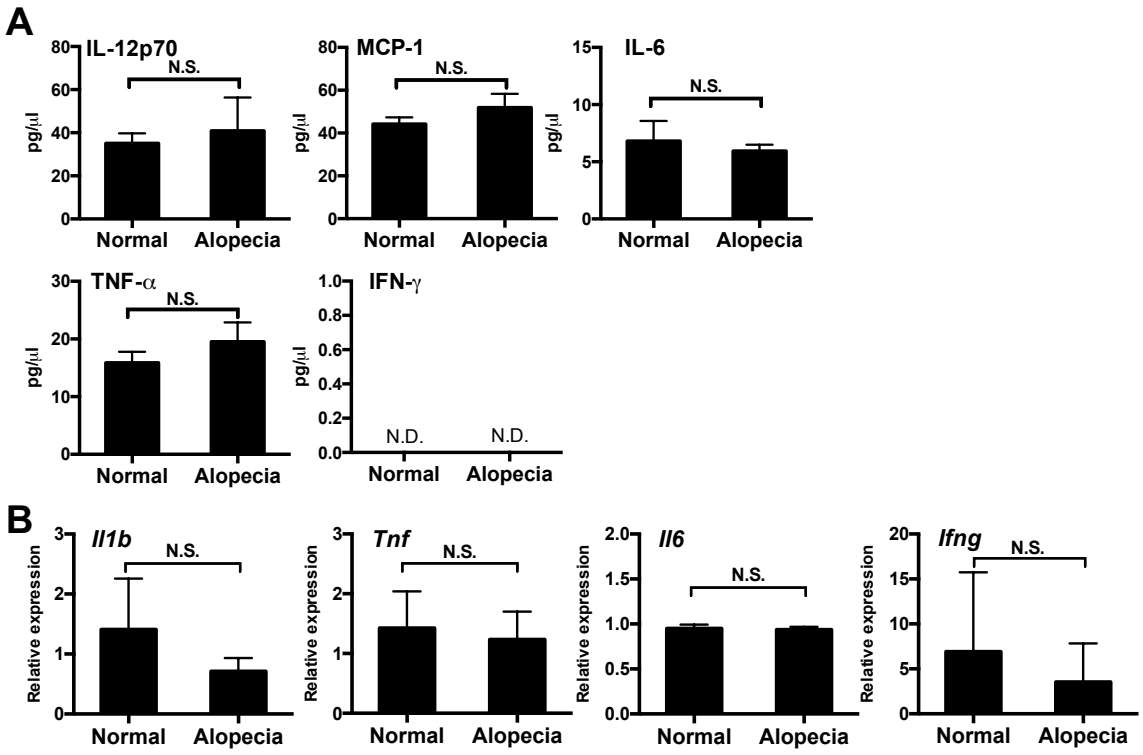
A
IL-12p70
MCP-1
IL-6
TNF-α
IFN-γ
pg/μl
N.S.
N.D.
Normal
Alopecia
B
Il1b
Tnf
Il6
Ifng
Relative expression
N.S.
Normal
Alopecia

**Figure S1. Alopecic mice did not increase pro-inflammatory cytokine, related to Figure 1**

Alopecic mice were induced by feeding a biotin deficient diet and treatment with vancomycin for 10 weeks. Pro-inflammatory cytokine production in the serum was measured by cytometric bead array (CBA) assay **(A).** Expression of the indicated mRNA in the skin, normalized to Act-b expression **(B)**. Statistical data are expressed as the mean ± standard error of mean. N.D., not detected. N.S., not significant.

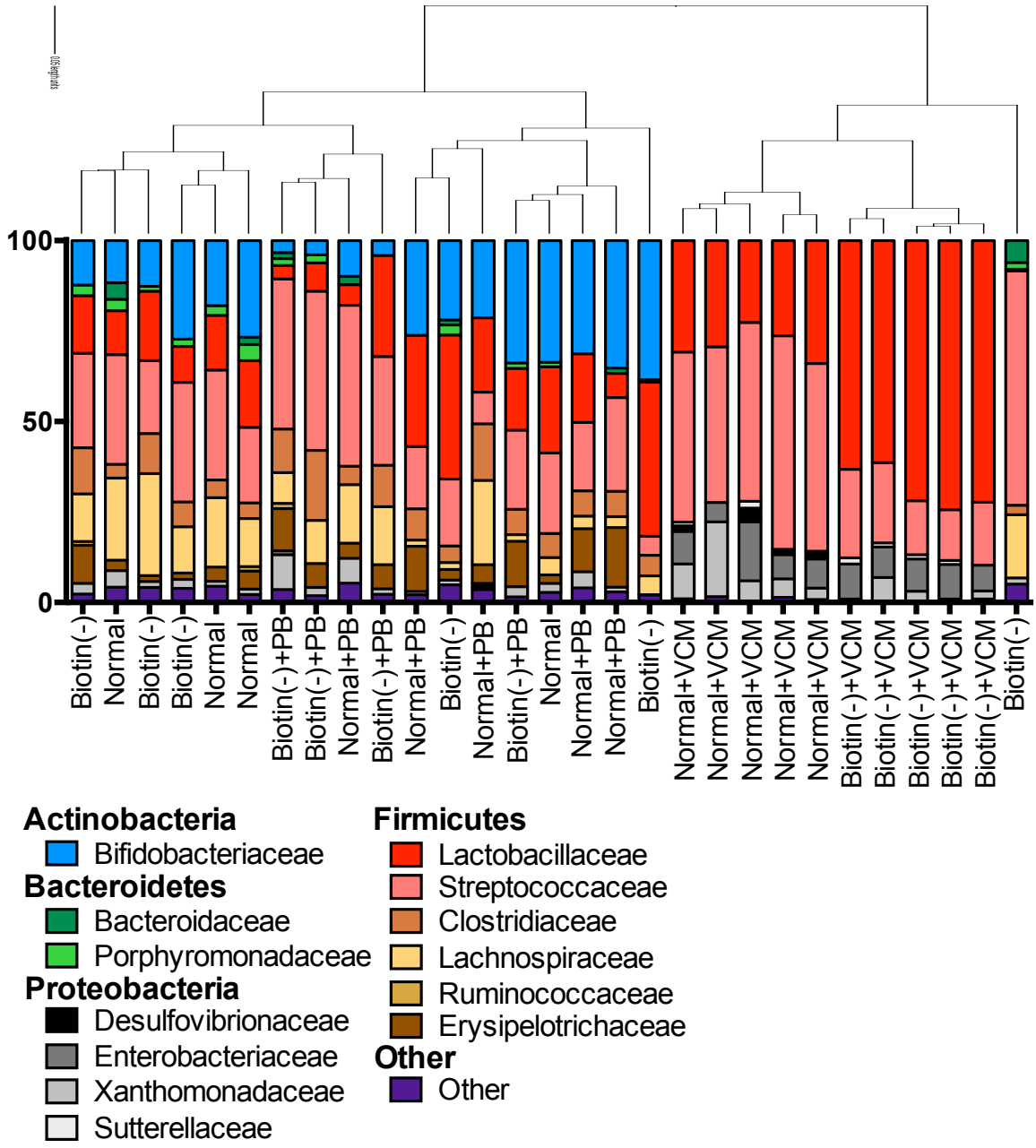
100
50
0
Biotin(-)
Normal
Biotin(-)
Biotin(-)
Normal
Normal
Biotin(-)+PB
Biotin(-)+PB
Normal+PB
Biotin(-)+PB
Normal+PB
Biotin(-)
Normal+PB
Biotin(-)+PB
Normal
Normal+PB
Normal+PB
Biotin(-)
Normal+VCM
Normal+VCM
Normal+VCM
Normal+VCM
Normal+VCM
Biotin(-)+VCM
Biotin(-)+VCM
Biotin(-)+VCM
Biotin(-)+VCM
Biotin(-)+VCM
Biotin(-)
Actinobacteria
Bifidobacteriaceae
Bacteroidetes
Bacteroidaceae
Porphyromonadaceae
Proteobacteria
Desulfovibrionaceae
Enterobacteriaceae
Xanthomonadaceae
Sutterellaceae
Firmicutes
Lactobacillaceae
Streptococcaceae
Clostridiaceae
Lachnospiraceae
Ruminococcaceae
Erysipelotrichaceae
Other
Other

**Figure S2. Alopecia mice showed increase of *Lactobacillaceae* abundance, related to Figure 2**

Microbiota composition from feces were analyzed via 16S rRNA analysis. Taxon-based analysis at family level among the groups. Data are shown as percent relative abundance.


L._satsumensis_AB154519
L._vini_AJ576009
L._nagelii_Y17500
L._mali_M58824
L._saerimneri_AY255802
L._acidipiscis_AB023836
L._aviarius_M58808
L._salivarius_DQ901733
L._equi_AB048833
L._agilis_M58803
L._ruminis_M58828
L._murinus_AJ621554
Isolated_strain
L._apodemi_AJ871178
L._animalis_M58807
L._algidus_AB033209
L._fuchuensis_AB063479
L._sakei_AY204893
L._curvatus_AM113777
L._graminis_AM113778
L._rhamnosus_D16552
L._casei_D16551
L._zeae_D86516
L._paracasei_D79212
L._composti_AB268118
L._bifermentans_M58809
L._coryniformis_M58813
L._rennini_AJ576008
L._sanfrancisco_X76327
L._lindneri_X95421
L._homohiochii_AM113780
L._fructivorans_X76330
L._zymae_AJ632157
L._acidifarinae_AJ632158
L._namurensis_AM259118
L._spicheri_AJ534844
L._farraginis_AB262732
L._hilgardii_M58821
L._diolivorans_AF264701
L._parakefiri_AY026750
L._buchneri_M58811
L._parafarraginis_AB262734
L._parabuchneri_AY026751
L._kefiri_AJ621553
L._rossiae_AJ564009
L._siliginis_DQ168027
L._perolens_Y19167
L._paracollinoides_AB005739
L._harbinensis_AB196123
L._kunkeei_Y11374
L._pantheri_AF413523
L._sharpeae_M58831
L._manihotivorans_AF000162
L._collinoides_AB005893
L._brevis_M58810
L._hammesii_AJ632219
L._parabrevis_AM158249
L._paraplantarum_AJ306297
L._pentosus_D79211
L._plantarum_D79210
L._tucceti_AJ576006
L._versmoldensis_AJ496791
L._farciminis_M58817
L._nantensis_AY690834
L._mindensis_AJ313530
L._alimentarius_M58804
L._kimchii_AF183558
L._paralimentarius_AJ417500
L._concavus_AY683322
L._dextrinicus_D87679
L._oligofermentans_AY733084
L._suebicus_AJ575744
L._vaccinostercus_AM113786
L._antri_AY253659
L._oris_X94229
L._reuteri_X76328
L._frumenti_AJ250074
L._panis_X94230
L._vaginalis_AF243177
L.pontis_X76329
L._mucosae_AF126738
L._ingluviei_AF333975
L._gastricus_AY253658
L._fermentum_AJ575812
L._coleohominis_AM113776
L._secaliphilus_AM279150
L._amylophilus_M58806
L._amylotrophicus_AM236149
L._psittaci_AJ272391
L._gasseri_M58820
L._johnsonii_AJ002515
L._iners_Y16329
L._fornicalis_Y18654
L._delbrueckii_M58814
L._intestinalis_AJ306299
L._acetotolerans_M58801
L._kalixensis_AY253657
L._ultunensis_AY253660
L._gallinarum_AJ242968
L._helveticus_AM113779
L._amylolyticus_Y17361
L._hamsteri_AJ306298
L._acidophilus_M58802
L._kefiranofaciens_AJ575259
L._crispatus_Y17362
L._amylovorus_M58805
L._kitasatonis_AB107638
L._sobrius_AY700063
0.005 length units

**Figure S3. Phylogenetic tree of *Lactobacillus* species and isolated strain, based on 16S rRNA sequences, related to Figure 2**

The reference sequences of *Lactobacillus* species were retrieved from GenBank and aligned with 16S rRNA sequence of isolated strain using ClustalW. Phylogenic tree was obtained using Maximum Likelihood method within the MEGA v.6.

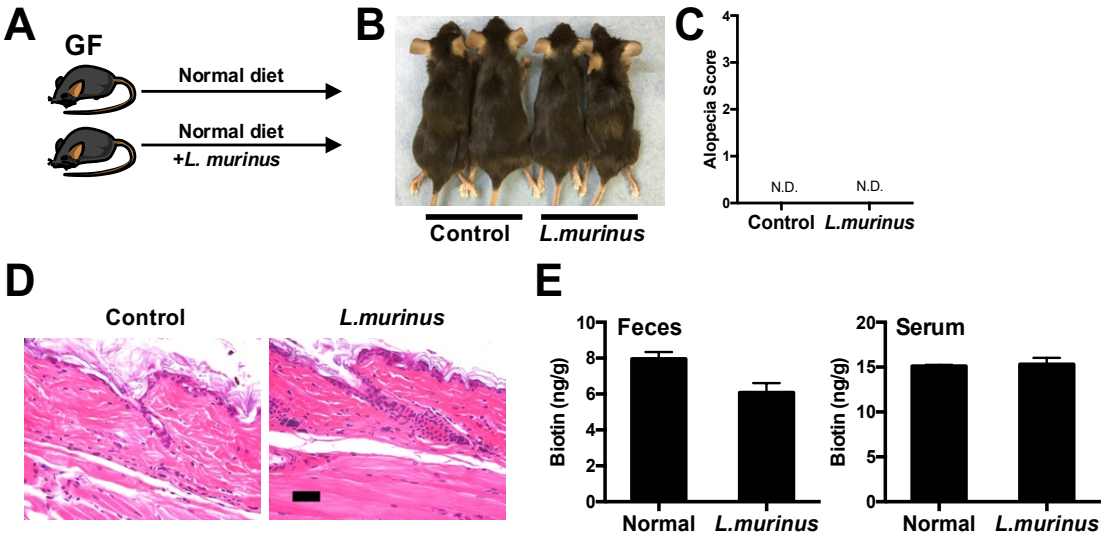
A
GF
Normal diet
Normal diet
+L. murinus
B
Control
L.murinus
C
Alopecia Score
4
3
2
1
0
N.D.
N.D.
Control
L.murinus
D
Control
L.murinus
E
Feces
Biotin (ng/g)
10
8
6
4
2
0
Normal
L.murinus
Serum
Biotin (ng/g)
20
15
10
5
0
Normal
L.murinus

**Figure S4. *L. murinus* mono-associaed mice fed normal diet did not induce alopecia, related to Figure 3**

**(A)** Experimental design. GF WT mice fed a normal diet were either untreated, or orally inoculated with *L.murinus* ($1\times10^8$ cells/200 μl). Representative macroscopic view of the skin **(B)**, alopecia score **(C)**, skin histology (H&E staining) **(D)**, and biotin concentration in feces and serum **(E)** of 2 groups.

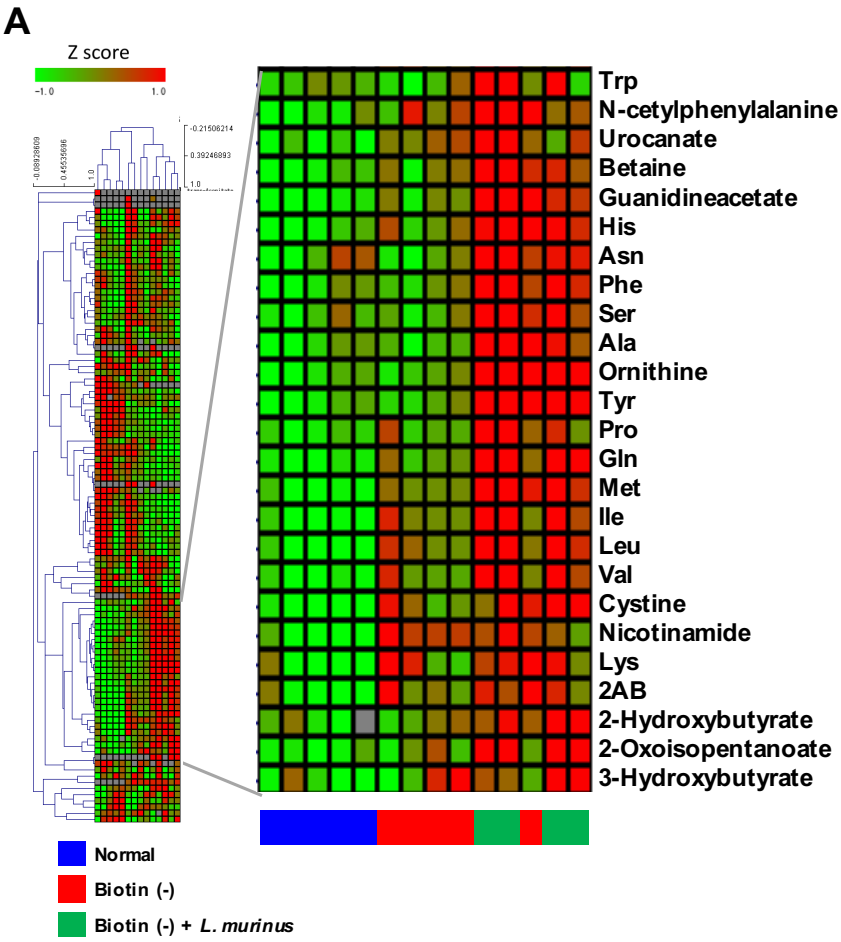
A
Z score
−1.0
1.0
Trp
N-cetylphenylalanine
Urocanate
Betaine
Guanidineacetate
His
Asn
Phe
Ser
Ala
Ornithine
Tyr
Pro
Gln
Met
Ile
Leu
Val
Cystine
Nicotinamide
Lys
2AB
2-Hydroxybutyrate
2-Oxoisopentanoate
3-Hydroxybutyrate
Normal
Biotin (-)
Biotin (-) + L. murinus

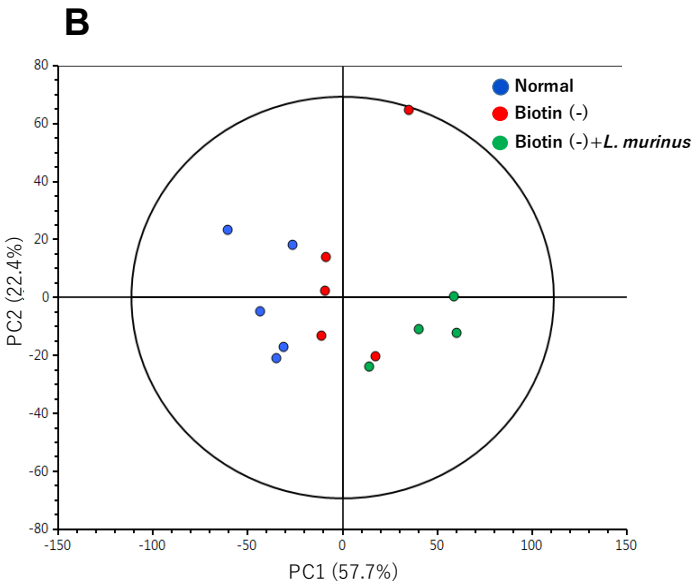
B
Normal
Biotin (-)
Biotin (-)+L. murinus
PC2 (22.4%)
PC1 (57.7%)

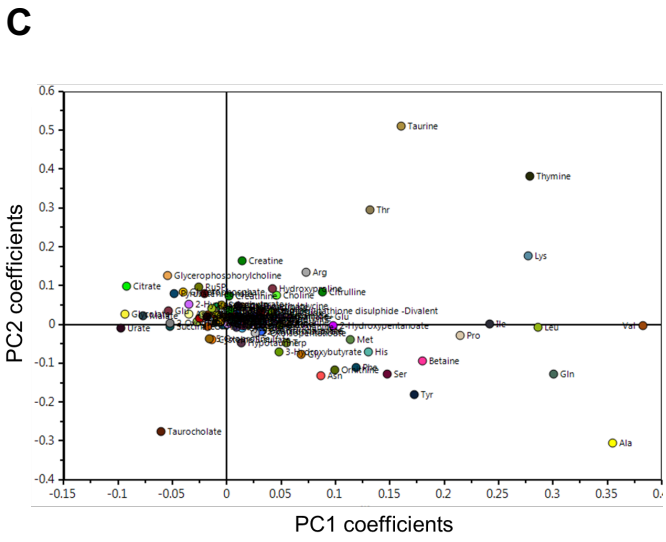
C
PC2 coefficients
PC1 coefficients
Taurine
Thymine
Thr
Lys
Creatine
Arg
Glycerophosphorylcholine
Citrate
Urate
Met
Pro
Ile
Leu
Val
Betaine
Gln
Ser
Tyr
Taurocholate
Ala

**Figure S5. Metabolic profiling of serum in GF and *L. murinus*-monocolnized mice fed with biotin deficient diet, related to Figure 3**

(A) The heatmap shows serum metabolome profiles measured by CE-TOFMS in GF mice fed normal and biotin deficient diet, and *L. murinus*-monocolnized mice fed with biotin deficient diet. HCA was run using a Pearson correlation metric and the average linkage method. Each row represents a metabolite; each column represents a mouse sample. The colors showed the average z score values calculated in all groups of mice. Gray columns indicate metabolites not detected in the mouse serum. CE-TOFMS-based metabolome analysis of serum in GF mice fed normal and biotin deficient diet, and *L. murinus* monocolonized mice fed with biotin deficient diet. The results of PCA on the metabolome data (B) and loading scatter plot (C) are shown. Proportions of the first (PC1) and second (PC2) principal components are 57.7% and 22.4%, respectively. The ellipse denotes the 95% significance limit of the model, as defined by Hotelling's t-test.

A

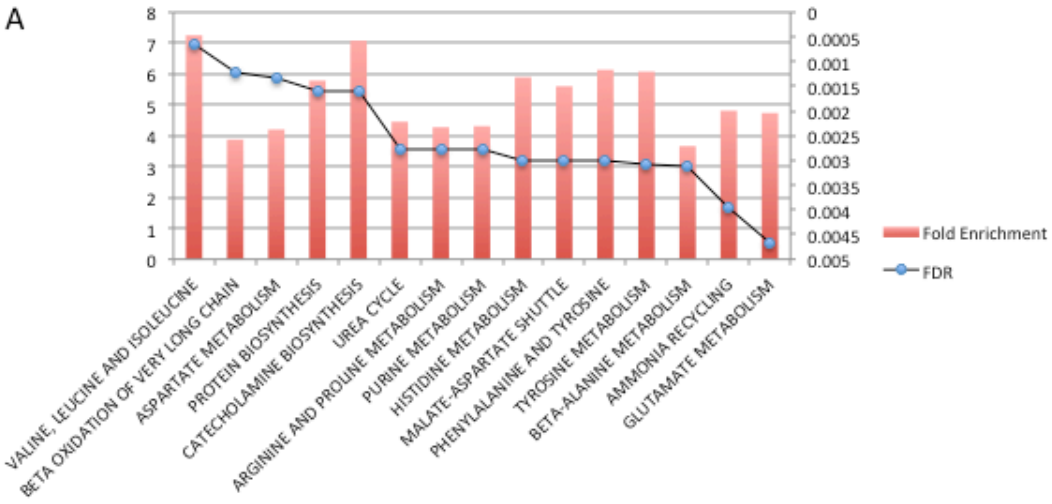
8
7
6
5
4
3
2
1
0
0
0.0005
0.001
0.0015
0.002
0.0025
0.003
0.0035
0.004
0.0045
0.005
Fold Enrichment
FDR
VALINE, LEUCINE AND ISOLEUCINE
BETA OXIDATION OF VERY LONG CHAIN
ASPARTATE METABOLISM
PROTEIN BIOSYNTHESIS
CATECHOLAMINE BIOSYNTHESIS
UREA CYCLE
ARGININE AND PROLINE METABOLISM
PURINE METABOLISM
HISTIDINE METABOLISM
MALATE-ASPARTATE SHUTTLE
PHENYLALANINE AND TYROSINE
TYROSINE METABOLISM
BETA-ALANINE METABOLISM
AMMONIA RECYCLING
GLUTAMATE METABOLISM

B

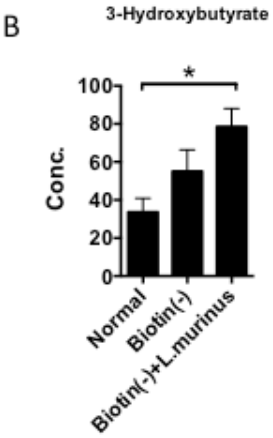
3-Hydroxybutyrate
*
100
80
60
40
20
0
Conc.
Normal
Biotin(-)
Biotin(-)+L.murinus

**Figure S6. Analysis of serum metabolites in GF and *L. murinus*-monocolnized mice fed with biotin deficient diet, related to Figure 3**

(A). Metabolite Set Enrichment Analysis (MSEA) of serum from normal (n=5) vs. biotin (-) + *L. murinus* (n=4). Enriched pathways (FDR < 0.005) were shown. (B and C). Concentration (μM) of branched chain amino acids (BCAA) and hydroxybutyrate is shown. (one-way ANOVA and subsequent Dunnett's multiple comparison test vs. normal group, *; $p < 0.05$)

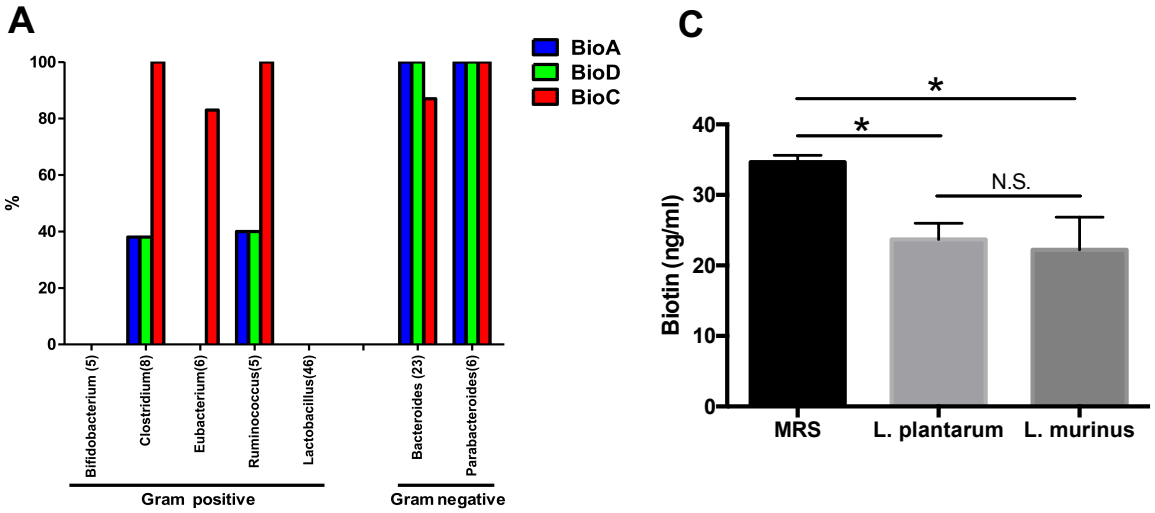
A
BioA
BioD
BioC
%
100
80
60
40
20
0
Bifidobacterium (5)
Clostridium(8)
Eubacterium(6)
Ruminococcus(5)
Lactobacillus(46)
Bacteroides (23)
Parabacteroides(6)
Gram positive
Gram negative
C
Biotin (ng/ml)
40
30
20
10
0
*
*
N.S.
MRS
L. plantarum
L. murinus

B

*L.murinus*

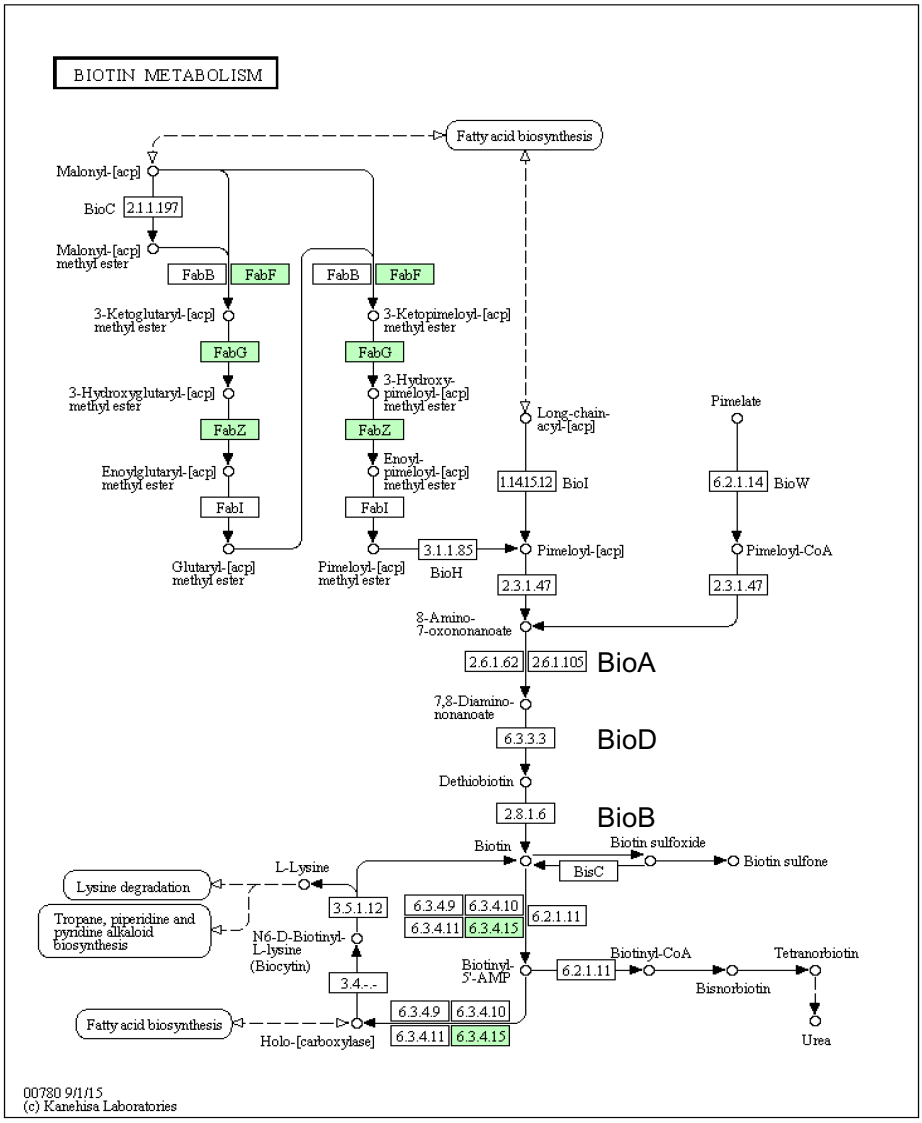
BIOTIN METABOLISM
Fatty acid biosynthesis
Malonyl-[acp]
BioC 2.1.1.197
Malonyl-[acp] methyl ester
FabB
FabF
FabB
FabF
3-Ketoglutaryl-[acp] methyl ester
3-Ketopimeloyl-[acp] methyl ester
FabG
FabG
3-Hydroxyglutaryl-[acp] methyl ester
3-Hydroxy-pimeloyl-[acp] methyl ester
FabZ
FabZ
Enoylglutaryl-[acp] methyl ester
Enoyl-pimeloyl-[acp] methyl ester
FabI
FabI
Long-chain-acyl-[acp]
Pimelate
1.14.15.12 BioI
6.2.1.14 BioW
Glutaryl-[acp] methyl ester
Pimeloyl-[acp] methyl ester
3.1.1.85 BioH
Pimeloyl-[acp]
Pimeloyl-CoA
2.3.1.47
2.3.1.47
8-Amino-7-oxononanoate
2.6.1.62
2.6.1.105
BioA
7,8-Diamino-nonanoate
6.3.3.3
BioD
Dethiobiotin
2.8.1.6
BioB
Biotin
Biotin sulfoxide
Biotin sulfone
BisC
L-Lysine
Lysine degradation
Tropane, piperidine and pyridine alkaloid biosynthesis
3.5.1.12
6.3.4.9
6.3.4.10
6.3.4.11
6.3.4.15
6.2.1.11
N6-D-Biotinyl-L-lysine (Biocytin)
Biotinyl-5'-AMP
6.2.1.11
Biotinyl-CoA
Tetranorbiotin
Bisnorbiotin
3.4.-.-
Fatty acid biosynthesis
6.3.4.9
6.3.4.10
6.3.4.11
6.3.4.15
Holo-[carboxylase]
Urea
00780 9/1/15
(c) Kanehisa Laboratories

**Figure S7. *L. murinus* lacks biotin synthesis genes and consumes the biotin, related to Figure 4**

(A) The biotin biosynthetic pathway involves the synthesis of three genes: 7,8-diaminonopelargonic acid (DAPA) synthase (BioA), dethiobiotin (DTB) synthase (BioD) and biotin synthase (BioB). The difference between the biosynthetic pathway genes of Gram-negative bacteria and Gram-positive bacteria analyzed by KEGG database. (B) Biotin metabolism pathway was obtained from the KEGG database. Green boxes are KEGG enzymes coded for by biotin metabolic and biosynthetic genes in *L. murinus*. KEGG enzyme 2.6.1.62 is coded for by bioA, KEGG enzyme 6.3.3.3 is coded for by bioD, KEGG enzyme 2.8.1.6 is coded for by bioB. (C) *L. plantarum* ATCC 8014 and *L. murinus* isolated from alopecic mice feces were aerobically cultured in fresh MRS broth at 37°C for 16h. The biotin level in supernatants were measured using Biotin Assay Medium (Nissui). N.S., not significant. *; $p < 0.05$

| Score | % of Hair Loss |
|---|---|
| 0 | Hair loss on 0 % of body |
| 1 | Hair loss on 1-10 % of body |
| 2 | Hair loss on 10-25 % of body |
| 3 | Hair loss on 25-50 % of body |
| 4 | Hair loss on 50-75 % of body |
| 5 | Hair loss on >75 % of body |
| 6 | Hair loss on 100 % of body |

**Table S1. Alopecia Score, related to Figure 1**

Alopecia was scored visually according to a 0–6 scoring system.

| KEGG ID | COMPOUND | KEGG ID | COMPOUND |
|---|---|---|---|
| C03626 | ADMA | C00711 | Malate |
| C00041 | Ala | C00383 | Malonate |
| C00956 | alpha-Aminoadipate | C00073 | Met |
| C00020 | AMP | C00879 | Mucate |
| C01262 | Anserine | C01042 | N-Acetylaspartate |
| C00062 | Arg | C00624 | N-Acetylglutamate |
| C00152 | Asn | C03519 | N-Acetylphenylalanine |
| C00049 | Asp | C01026 | N,N-Dimethylglycine |
| C08261 | Azelate | C03793 | N6,N6,N6-Trimethyllysine |
| C00099 | beta-Ala | C00153 | Nicotinamide |
| C00719 | Betaine | C02571 | o-Acetylcarnitine |
| C00318 | Carnitine | C00077 | Ornithine |
| C00114 | Choline | C00295 | Orotate |
| C00417 | cis-Aconitate | C00074 | PEP |
| C02614 | Citramalate | C00079 | Phe |
| C00158 | Citrate | C00408 | Pipecolate |
| C00327 | Citrulline | C00148 | Pro |
| C00300 | Creatine | C00022 | Pyruvate |
| C00791 | Creatinine | C00199 | Ru5P |
| C05824 | Cysteine S-sulfate | C00818 | Saccharate |
| C00491 | Cystine | C00065 | Ser |
| C00475 | Cytidine | C00780 | Serotonin |
| C00380 | Cytosine | C00042 | Succinate |
| C00111 | DHAP | C00898 | Tartrate |
| C00122 | Fumarate | C00245 | Taurine |
| C00092 | G6P | C05122 | Taurocholate |
| C01181 | gamma-Butyrobetaine | C00188 | Thr |
| C00064 | Gln | C03618 | threo-beta-methylaspartate+Glu |
| C00025 | Glu | C01620 | Threonate |
| C00329 | Glucosamine | C00178 | Thymine |
| C00191 | Glucuronate | C02341 | trans-Aconitate |
| C00489 | Glutarate | C01104 | Trimethylamine N-oxide |
| C00127 | Glutathione(ox) | C00078 | Trp |
| C00037 | Gly | C00082 | Tyr |

| | | | |
|---|---|---|---|
| C00093 | Glycerophosphate | C00105 | UMP |
| C00670 | Glycerophosphorylcholine | C00366 | Urate |
| C00160 | Glycolate | C00086 | Urea |
| C00144 | GMP | C00785 | Urocanate |
| C00581 | Guanidinoacetate | C00183 | Val |
| C01585 | Hexanoate | C02918 | 1-Methylnicotinamide |
| C00135 | His | C05984 | 2-Hydroxybutyrate |
| C00263 | Homoserine | C02630 | 2-Hydroxyglutarate |
| C01015 | Hydroxyproline | C00026 | 2-Oxoglutarate |
| C00519 | Hypotaurine | C00141 | 2-Oxoisopentanoate |
| C00407 | Ile | C00881 | 2'-Deoxycytidine |
| C05123 | Isethionate | C02356 | 2AB |
| C00311 | Isocitrate | C01089 | 3-Hydroxybutyrate |
| C00186 | Lactate | C01152 | 3-Methylhistidine |
| C00123 | Leu | C00197 | 3PG |
| C00047 | Lys | C01879 | 5-Oxoproline |

**Table S2. List of metabolites used for MSEA analysis, related to Figure 3**

| Ingredient | AIN-93G | Modified AIN-93G (Biotin deficient) |
|---|---|---|
| Casein | 20.00 | 20.00 |
| L-Cystine | 0.30 | 0.30 |
| Cornstarch | 39.7486 | 39.7486 |
| Dextrinizaed cornstarch | 13.20 | 13.20 |
| Sucrose | 10.00 | 10.00 |
| Soybean oil | 7.00 | 7.00 |
| Cellulose powder | 5.00 | 5.00 |
| AIN-93G Mineral mix | 3.50 | 3.50 |
| AIN-93 Vitamin mix | 1.00 | - |
| Modified Vitamin mix | - | 1.00 |
| Choline bitartrate | 0.25 | 0.25 |
| Tert-butylhydroquinone | 0.0014 | 0.0014 |
| Total | 100.00 | 100.00 |
| | | g/100g diet |

| Vitamin | AIN-93 vitamin mix | Modified vitamin mix |
|---|---|---|
| Vitamin A (all-trans-retinyl palmitate) 325,000IU/g | 0.12308 | 0.12308 |
| Vitamin $D_3$ (cholecalciferol) 100,000IU/g | 0.10000 | 0.10000 |
| Vitamin E (all-rac-α-tocopheryl acetate) 50% | 1.50000 | 1.50000 |
| Thiamin-HCl | 0.06000 | 0.06000 |
| Riboflavin | 0.06000 | 0.06000 |
| Pyridoxine-HCl | 0.07000 | 0.07000 |
| Vitamin B12 (cyanocobalamin) 0.1% | 0.25000 | 0.25000 |
| Vitamin K (phylloquinone) | 0.00750 | 0.00750 |
| D-Biotin | 0.00200 | - |
| Folic acid | 0.02000 | 0.02000 |
| Ca Pantothenate | 0.16000 | 0.16000 |
| Nicotinic acid | 0.30000 | 0.30000 |
| Sucrose | 97.34742 | 97.34942 |
| Total | 100.00000 | 100.00000 |
| | | g/100g mix |

**Table S3. Diet composition data, related to Figure 1**

Experimental diets composition both AIN93G and AIN93G without biotin.

## SUPPLEMENTAL EXPERIMENTAL PROCEDURES

### Quantitative Real-Time PCR

qPCR analysis was performed using SYBR Premix EX Taq and the Thermal Cycler Dice Real Time System II (TAKARA). The primer sets used in this study were as follows: total *Lactobacillus* forward 5′-TGGAAACAGRTGCTAATACCG-3′ and reverse 5′-GTCCATTGTGGAAGATTCCC-3′; *L. murinus* forward 5′-AGCTAGTTGGTGGGGTAAAG-3′ and reverse 5′-TAGGATTGTCAAAAGATGTC-3′.

### Functional gene annotation

The sequencing library of *L. murinus* was constructed with the NEBNext DNA Library Prep Master Mix Set for Illumina (New England Biolabs) and sequenced on a Miseq sequencer using paired 300-bp reads with Miseq Reagent Kit V3. The genome was assembled using Platanus 1.2.1 (Kajitani et al., 2014). Rapid Annotation using Subsystem Technology (RAST) was used for gene annotation (Aziz et al., 2008). Functional annotation was performed using the KEGG (Kanehisa and Goto, 2000).

### Purification of total RNA from mouse skin and RT-qPCR

The RNeasy fibrous tissue mini kit (Qiagen) was used for purification of total RNA from the skin according to the manufacturer's instructions. Complementary DNA was synthesized from 100 ng of total RNA using TaqMan Reverse Transcription Reagents (Applied Biosystems). Reverse transcription was performed at 25°C for 10 min, 48°C for 30 min, and then 95°C for 5 min each cycle. Complementary DNA was analyzed by RT-PCR using the TaqMan Universal PCR Master Mix (Applied Biosystems) in the Applied Biosystems StepOne ™ / StepOnePlus ™ (Applied Biosystems). The following probes were purchased from Applied Biosystems: IL-1b (00434228_m1), IL-6 (00446190_m1), Ifng (99999071_m1) and Tnf (00443258_m1).

### In vitro assay of biotin consumption

*L. plantarum* ATCC 8014 and *L. murinus* isolated from alopecic mice feces were aerobically cultured in fresh MRS broth at 37°C for 16h. The samples were centrifuged at 10,000 g for 10 min, and the supernatants were

filtered through a 0.45μm filter. Biotin concentration was measured from supernatants using Biotin Assay Medium (Nissui).

**Cytokine Assay**

A mouse inflammatory cytometric bead array (CBA) kit (BD Biosciences) was used for cytokine measurements, according to the manufacturer's instructions. Samples were analyzed with a FACS Canto II flow cytometer (BD Biosciences).

**CE-TOFMS Measurement**

Quantitative analysis of charged metabolites by CE-TOFMS was performed as described previously (Mishima et al., 2015). CE-TOFMS experiments were performed using the Agilent CE System (Agilent Technologies), the G1603A Agilent CE-MS adapter (Agilent Technologies), and the G1607A Agilent CE-ESI-MSSprayer Kit. PCA and HCA on the serum metabolome data were run with the SIMCA-P+ software (ver 12.0, Umetrics) and MultiExperiment Viewer (MeV) version 4.8.1 software (Dana-Farber Cancer Institute, Harvard Medical School, Boston, MA, USA), respectively.

**Metabolite set enrichment analysis (MSEA)**

MSEA was performed by MetaboAnalyst 3.0 as described previously (Xia and Wishart, 2011). One hundred metabolites with KEGG ID (Table3) were used to calculate the enrichment. The bar length is based on the fold enrichment calculated as calculated statistic / expected statistic plotted with p value.

**Electron Microscopy**

Electron microscopic studies were performed as previously described (Hayashi et al., 2013). Briefly, dissected 0.5 cm colon tissue samples were cut open and fixed with 2% paraformaldehyde/2% glutaraldehyde in 0.1 M phosphate buffer (pH 7.4) at 4°C overnight. The samples were fixed with 2% osmium tetroxide in 0.1 M

phosphate buffer at 4°C for 2 h, transferred into tert-butyl alcohol 3 times for 30 min each, and frozen at 4°C. After drying, the samples were observed using a scanning electron microscope (S-800, Hitachi).

**SUPPLEMENTAL REFERENCES**

Aziz, R.K., Bartels, D., Best, A.A., DeJongh, M., Disz, T., Edwards, R.A., Formsma, K., Gerdes, S., Glass, E.M., Kubal, M.*, et al.* (2008). The RAST Server: rapid annotations using subsystems technology. BMC Genomics *9*, 75.

Hayashi, A., Sato, T., Kamada, N., Mikami, Y., Matsuoka, K., Hisamatsu, T., Hibi, T., Roers, A., Yagita, H., Ohteki, T.*, et al.* (2013). A single strain of Clostridium butyricum induces intestinal IL-10-producing macrophages to suppress acute experimental colitis in mice. Cell Host Microbe *13*, 711-722.

Kajitani, R., Toshimoto, K., Noguchi, H., Toyoda, A., Ogura, Y., Okuno, M., Yabana, M., Harada, M., Nagayasu, E., Maruyama, H.*, et al.* (2014). Efficient de novo assembly of highly heterozygous genomes from whole-genome shotgun short reads. Genome Res *24*, 1384-1395.

Kanehisa, M., and Goto, S. (2000). KEGG: kyoto encyclopedia of genes and genomes. Nucleic Acids Res *28*, 27-30.

Mishima, E., Fukuda, S., Shima, H., Hirayama, A., Akiyama, Y., Takeuchi, Y., Fukuda, N.N., Suzuki, T., Suzuki, C., Yuri, A.*, et al.* (2015). Alteration of the Intestinal Environment by Lubiprostone Is Associated with Amelioration of Adenine-Induced CKD. J Am Soc Nephrol *26*, 1787-1794.

Xia, J., and Wishart, D.S. (2011). Web-based inference of biological patterns, functions and pathways from metabolomic data using MetaboAnalyst. Nat Protoc *6*, 743-760.